THE PENNSYLVANIA STATE UNIVERSITY
SCHREYER HONORS COLLEGE

DEPARTMENT OF BIOENGINEERING

THE USE OF TIME CORRELATED SINGLE PHOTON COUNTING TO OPTIMIZE siRNA ENCAPSULATION IN NANOLIPOSOMES

ELAINE TANELLA
Spring 2012

A thesis
submitted in partial fulfillment
of the requirements
for a baccalaureate degree
in Bioengineering
with honors in Bioengineering

Reviewed and approved* by the following:

Peter Butler
Associate Professor of Bioengineering
Thesis Supervisor & Honors Advisor

Margaret J. Slattery
Assistant Professor of Bioengineering
Faculty Reader

* Signatures are on file in the Schreyer Honors College.

ABSTRACT

Short interfering RNA (siRNA) mediates gene silencing in mammalian cells. The potential of this molecule to serve as a therapeutic agent for disease such as cancer is currently being examined. In order to be effective, siRNA must interact with the target cell's RNA machinery found in its cytoplasm. However, siRNA, being negatively charged, cannot spontaneously enter a cell's cytoplasm due to the nature of the phospholipid bilayer. Additionally, the stability of siRNA is questionable due to the fact that it can be easily degraded by RNAases naturally found in the human body. These problems could be solved by utilizing nanoliposomes as vehicles to transport siRNA to a targeted tumor cell area, bypassing extracellular RNAses.

This project uses time-correlated single photon counting (TCSPC) to perform fluorescence correlation spectroscopy (FCS) and to determine molecular brightness (MB) values of fluorescently-tagged siRNA molecules in order to measure the encapsulation efficiency of nanoliposome-siRNA encapsulation. Using this method, the following quantitative information can be extracted from the nanoliposome-siRNA samples: diffusion coefficient (τD), hydrodynamic radii (R), and average concentration (C). TCSPC allows all of this information to be obtained by one system instead of multiple systems.

We found that siRNA was able to be encapsulated into the fabricated nanoliposomes, though the quantity of siRNA in each nanoliposome varied. Additionally, we found that TCSPC was an ideal method to obtain multiple important characteristics of these siRNA-nanoliposomes simultaneously.

TABLE OF CONTENTS

LIST OF FIGURES

LIST OF TABLES

ACKNOWLEDGEMENTS

I have been very fortunate to receive support from numerous individuals while completing this thesis work. First, I would like to thank Dr. Peter Butler for providing me with an opportunity to get involved in nanomedicine research, and for guiding me with this research over the past two years.

I would also like to thank Dr. Maggie Slattery for her guidance and mentorship throughout my undergraduate career. She has been an incredible support system, and a critical person to my success at Penn State.

Lastly, I would like to thank my family and friends for their support throughout this entire process. I am extremely fortunate to have had such amazing individuals by my side throughout my undergraduate years.

Chapter 1

Introduction

1.1 Cancer

Cancer is defined as the abnormal growth of cells that is a result of gene expression changes. These changes cause an imbalance between cell proliferation and death, and ultimately lead to a population of cells that could potentially metastasize to other tissues within the body (Jemal et al. 2010).

According to the American Cancer Society, more than 1,500 people die from cancer each day in the United States. However, the primary cause of cancer mortality is not caused directly by the formation of a tumor; it is caused by the metastases of this cancer to distant organ sites (Dittmar et al. 2008). Thus, the need is great for developing an effective method for treating and targeting cancer.

1.2 Current Cancer Treatments

The three main types of cancer treatments are chemotherapy, radiation and surgery. Radiation therapy uses high-energy radiation through x-rays, gamma rays, and other charged particles, to shrink tumors and kill cancer cells. A patient can undergo radiation treatment through external-beam radiation therapy, received external of the body, internal radiation therapy, received internally, or through systemic radiation therapy, internally through the circulatory system. Radiation kills cancer cells by damaging DNA, causing these cancer cells to eventually undergo apoptosis (Jemal et al. 2010), (Dittmar et al. 2008).

Both radiation and chemotherapy can have many side effects since they are not always targeted therapies. Side effects from radiation therapy can include skin irritation, salivary gland

damage, hair loss, nausea, urinary problems, fibrosis, memory loss, and infertility. Chemotherapy is a systemic treatment, and more than 100 different drugs are currently used today for chemotherapy. These chemotherapy drugs target cells in a specific phase of the cell cycle. These drugs target cells that are in an actively dividing phase, since cancer cells divide uncontrollably (Jemal et al. 2010), (Dittmar et al. 2008). Unfortunately, chemotherapy drugs cannot differentiate between normal tissue cells that are actively dividing, or cancer cells. Thus, there are many side effects associated with chemotherapy treatment that include bone marrow suppression, nervous system changes, low white blood cell counts, hair loss, sores in the mouth and throat, taste changes, diarrhea, fatigue, and heart damage (Jemal et al. 2010).

1.3 Short Interfering RNA

Short interfering RNA or (siRNA) is chemically synthesized double stranded RNA that contains approximately19-23 nucleotides, and is 7.5 nm in length (Schroeder et al. 2009). Two nucleotides remain unpaired in the 5'-phosphorylated ends and unphosphorylated 3'end. One of the main downfalls with siRNA use is that it cannot directly be delivered to a cell, since it is almost instantaneously degraded in the body by naturally occurring RNAses (Semple et al. 2010) (Tokatlian and Segura. 2010).

siRNA can mediate gene silencing in mammalian cells. Once siRNA enters a cell, it assembles into an RNA-induced silencing complex (RISC) with nucleases and proteins. The RISC allows the antisense strand of siRNA to bind to the complementary sequence of mRNA, thus inducing degradation of the complementary mRNA. This process can be seen in Figure1.3.1. Ultimately, siRNA can be designed to target the mRNA of a protein that causes the cell to divide uncontrollably, stopping the growth of cancerous cells (Tokatlian and Segura. 2010). Once siRNA has entered a cell, the length of expression knockdown is between 3-7 days in dividing cells, and up to 3-4 weeks in dividing cells (Schroeder et al. 2009).

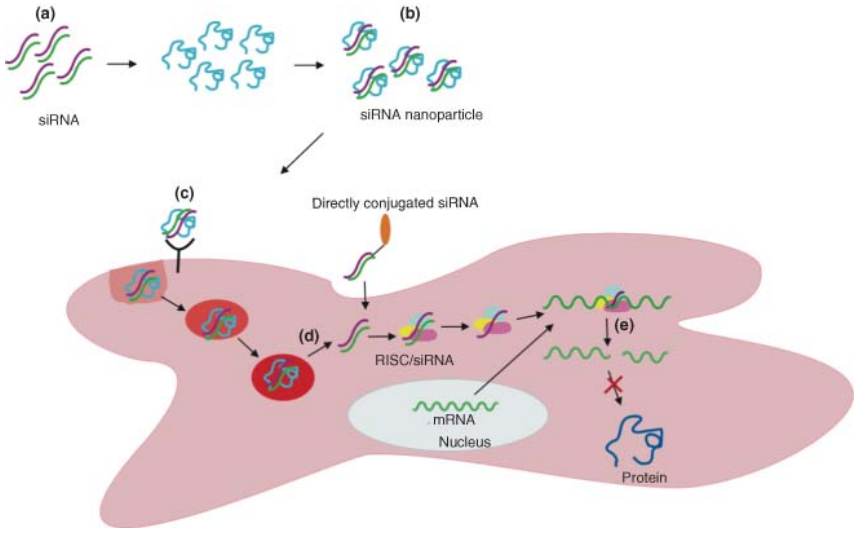

Figure 1.3.1 Schematic of the pathway to silencing a gene using siRNA. The siRNA (a) must use a vehicle, i.e. a nanoparticle (b), to enter the cell. When this nanoparticle binds to the appropriate cell-surface receptor (c), it is taken into the cell, and the siRNA is released into the cytoplasm (d) where it forms a RISC with nucleases and other proteins. The RISC allows the antisense strand of the siRNA to bind with the complementary sequence of mRNA (e), causing the degradation of that mRNA (e), and prevention of a certain protein forming (Tokatlian and Segura. 2010).

1.4 Time-Correlated Single Photon Counting

Time-correlated single photon counting (TCSPC) can be accomplished via a peripheral component interconnect card (PCI) and the use of continuous and pulsed wave lasers. Through the integration of these three items, nanosecond to second-scale dynamics can be determined from single fluorescent molecules. These dynamics can be analyzed using fluorescence correlation spectroscopy (FCS) and fluorescence lifetime (FL). These analysis methods can be used to determine information regarding diffusion, conformational changes, aggregation, and molecular size (Gullapalli et al. 2007).

The TCSPC detector signal is composed of randomly distributed pulses because it detects individual photons. There are often many signal events without photons, while other signal events contain one pulse from the photon. It is rare to see signal periods with more than one photon. TCSPC basically works as follows: First, one photon is detected and recorded as a fluorescent event. Second, the time that elapses between the arrival of the excitation pulse and the photon is captured. Then, the events are collected by adding a "1" with an address proportional to the detection time. After many photons have been detected, the distribution of the photons versus time builds up. Figure 1.4.1 below displays the way TCSPC counting data is collected (Becker. 2008).

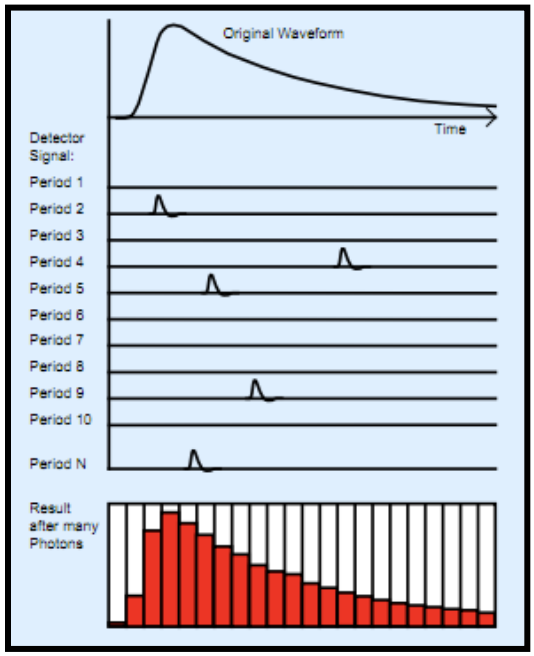

Figure 1.4.1 TCSPC Measurement Principle. Single photons are collected during different time periods. Some time periods have no photons (Becker. 2008).

1.5 Fluorescence Correlation Spectroscopy

Fluorescence Correlation Spectroscopy is a sensitive analytical tool that is based on exciting a small number of molecules in a tiny volume, about one femtoliter, and correlating the

fluctuations of the fluorescence intensity. These fluctuations are caused by diffusion, rotation, conformational changes, and other effects (Becker. 2008).

As particles flow across the confocal volume, they fluoresce. The light from the fluorescence of the particle is collected by the objective lens. Since the fluoresced light is red-shifted with respect to the excitation light, it passes through the dichroic mirror reaching the photon multiplier tube (PMT). The electronic signal received after it passes through the PMT can be stored directly as an intensity versus time plot, or directly computed to generate an autocorrelation curve. A tiny confocal volume, as seen in Figure 1.5.1 contains a small number of fluorescent particles (Gullapalli et al. 2007). If there are multiple molecules fluorescing at once, the plot becomes difficult to read, and it is hard to determine which fluctuations are based upon an individual molecule. Therefore, a solution in the nanomolar range must be used in order to decrease the number of molecules present in the confocal volume at any one time.

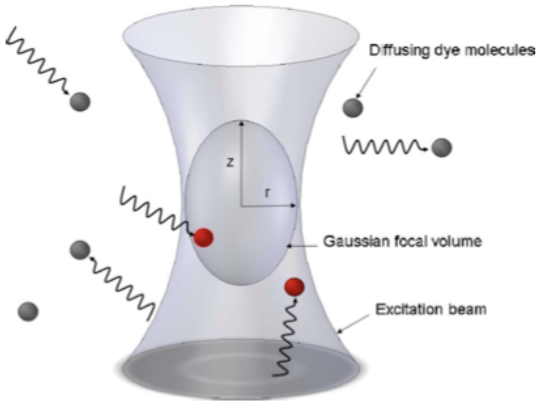

Figure 1.5.1 Confocal Volume for FCS. Fluorescent molecules are excited by the laser beam, and fluorescence emission is only collected in the Gaussian confocal volume(Gullapalli et al. 2007).

The analysis of these fluctuations by autocorrelation can provide information regarding diffusion coefficients, as well as other information about properties of single molecules. The

relationship between autocorrelation, fluctuations, and molecular diffusion can be analyzed to determine these key properties. The Stokes-Einstein relationship is as follows:

$$D = \frac{k_b T}{6\pi\eta R}, \tag{1}$$

where k_b is the Boltzmann constant, T is the absolute temperature, D is the diffusion coefficient of a sphere with a hydrodynamic radius R in a solvent of viscosity η. The 2D characteristics of molecular diffusion can be defined as:

$$r^2 = 4D\tau_D, \tag{2}$$

where τ_D is the molecular diffusion transition time, and r is the radius of a small area. At equilibrium, fluorescence intensity fluctuates around an average $\langle F \rangle$. The intensity of these fluctuations (δF(t)), can be autocorrelated to form the equation below:

$$G(\tau) = \frac{\langle \delta F(t+\tau)\delta F(t)\rangle}{\langle \delta F(t)\rangle^2}, \tag{3}$$

where t is time and τ is lag time that varies over all of the times during the collection period. The autocorrelation function in relation to the Gaussian confocal volume is defined as

$$G(\tau) = \frac{1}{N}\left[\frac{1}{1+(\frac{\tau}{\tau_D})}\right]\left[\frac{1}{1+\left(\frac{1}{\omega}\right)^2(\frac{\tau}{\tau_D})}\right]^{1/2} \text{(Gullapalli et al. 2007)}, \tag{4}$$

where ω is the height of the confocal volume divided by the width and N is the average number of molecules in the confocal volume. Figure 1.5.2 below shows the development of an autocorrelation curve.

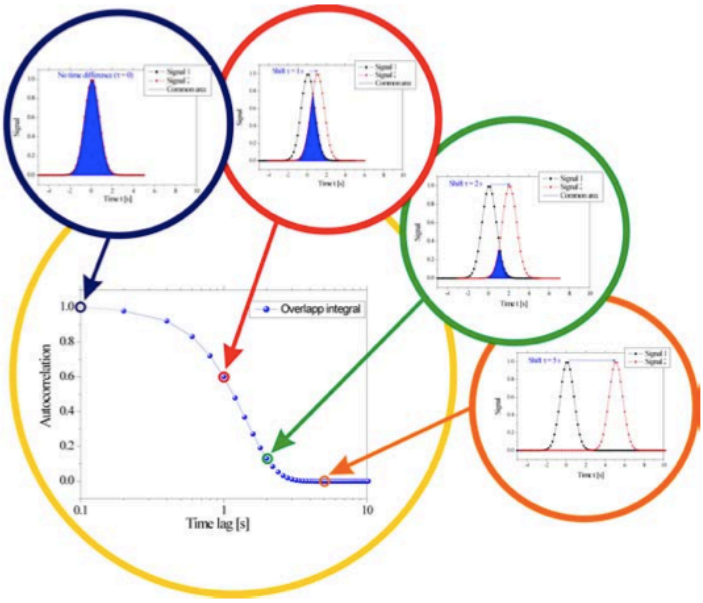

Figure 1.5.2 Development of an autocorrelation curve from FCS data (Schwille and Haustein. 2009)

1.6 Molecular Brightness

The molecular brightness, with units of counts/second, is calculated by the following equation:

$$MB = \frac{\langle F(t) \rangle}{N} = \langle F(t) \rangle \cdot G(0) \quad \text{(Schwille and Haustein. 2009),} \qquad (5)$$

where F(t) is the average fluorescence count rate, N is the number of molecules in the confocal volume, and G is the autocorrelation function. Molecular brightness is important to these experiments because it will ultimately help us determine the encapsulation efficiency of nanoliposomes. These details are discussed in Chapter 2.

1.7 Dynamic Light Scattering

Dynamic Light Scattering is technique that measures the speed at which particles move under Brownian motion. It is used to characterize the size of various particles including proteins, polymers, and nanoparticles. This technique works by comparing fluctuations in intensity of

scattered light at one point in time, and comparing these with measurements at later times. The fluctuations are measured for a short period of time and multiplied by the fluctuations at a later point in time, providing a correlation for the signal over time (Maherani et al. 2011).

Correlations of successive time points are plotted against the time shift, resulting in a function that is inversely exponential. The rate of the exponential decay is inversely proportional to the size of the particles since smaller particles move faster. The radius of particles can be calculated by rearranging the Stokes-Einstein equation, as seen in Equation (1) below (Maherani et al. 2011).

1.8 Nanoliposome Properties

Nanoliposomes were first developed when it was discovered that phospholipids would spontaneously form spherical closed structures when placed in an aqueous solutions. These phospholipids spontaneously form these spherical closed structures due to the amphipathic characteristics of phospholipids. The hydrophobic region of these phospholipids form layers, referred to as lamellae (Chrai et al. 2002).

Liposomes can vary in charge and in size depending on the lipids used in the formation technique. They can vary anywhere from 0.5-5.0 μm, and be unilamellar or multilamellar. Nanoscale liposomes have many advantages over larger liposomes. Nanoliposomes can remain in the human circulatory system for longer periods of time without being recognized by microphages. They can also travel through capillaries and biological membranes more easily because of their nanoscale size (Maherani et al. 2011).

The composition of nanoliposomes can determine the application of these particles. The types of lipids used to fabricate the nanoliposomes can affect biodistribution, surface charge, permeability, and the release of the carrier material. Single chain lipids were found to be able to form vesicles, but they are less efficient at encapsulating materials. Phospholipids are better at

forming vesicles and have a greater encapsulation efficiency (Maherani et al. 2011).

Another important component of liposome formulation are sterols. These molecules can affect the stability, fluidity, and permeability. Sterols can provide steric hindrance, and also electrostatic repulsion. Cholesterol is one of the most used sterols, and it is often used to prevent the formation of aggregates. Adding cholesterol to a bilayer also reduces the permeability of the membrane to solutes. The amount of sterols used in liposome formulation depends on the function of the vesicles (Maherani et al. 2011). It has been found that vesicles with greater than 10% composition of cholesterol are ineffective at incorporating DNA molecules (Mozafari. 2010).

Polyethylene glycol (PEG), a polyether compound, is often used on the surface of liposomes in order to promote long circulating times, improve the stability of the liposomes, and to also protect the encapsulated materials against degradation (Maherani et al. 2011). PEG is able to accomplish all of these things by lowering the adsorption of plasma proteins (Buyens et al. 2009).

siRNA can best be encapsulated in a nanoliposome by using cationic lipids, since they will bind to the negatively charged siRNA. Therapeutics involving siRNA require that the nanoliposomes:

(1) Protect siRNA from degradation during circulation

(2) Deliver siRNA to the target cells and do not deliver siRNA to non-target cells

(3) Promote cellular uptake and escape through the endosome

(4) Release siRNA intracellularly so that it is accessible to key cell machinery in the cytoplasm (Schroeder et al. 2009).

There are many ways that nanoliposomes can accomplish (4) from above. Nanoliposomes can specifically or nonspecifically adsorb onto the cell surface or fuse with the cell membrane, releasing their contents into the cell cytoplasm. Nanoliposomes can also be destabilized by

certain cell membrane components as they adsorb to the surface, and the siRNA can enter the cell by pinocytosis. Nanoliposomes can also be targeted to a specific cell for endocytosis, and be delivered to the lysosome, or can destabilize the endosome and release the siRNA into the cell cytoplasm (Torchilin. 2005). Figure 1.8.1 below displays these ways that nanoliposomes release siRNA intracellularly.

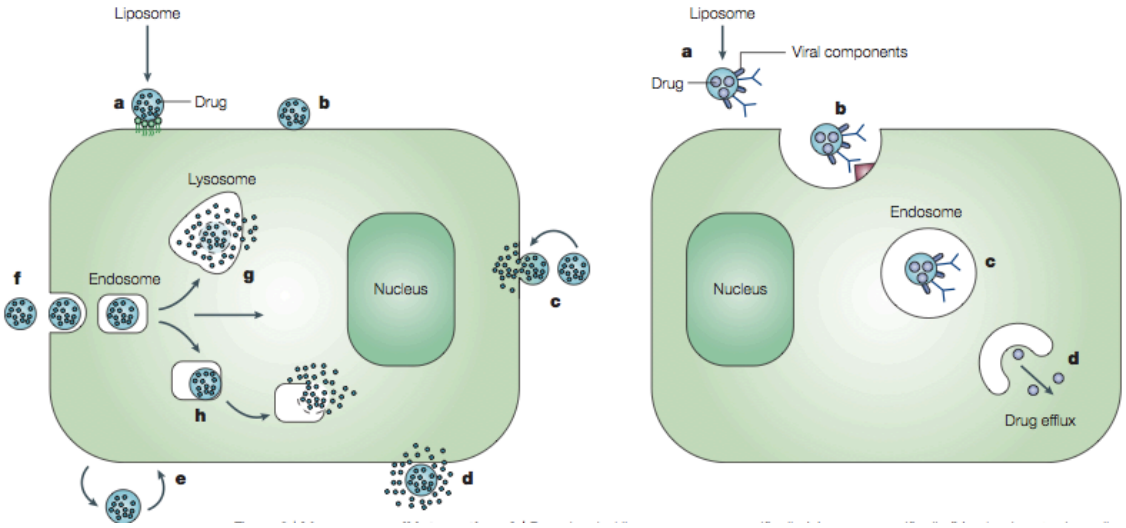

Figure 1.8.1 Different pathways that siRNA-nanoliposomes can enter a cell (Torchilin. 2005)

1.9 Nanoliposome Fabrication Techniques

There are currently many fabrication techniques for nanoliposomes, each with their advantages and disadvantages. One of the original techniques for liposome formation is the Bangham method, which involves the dissolution of lipids in an organ phase, removal of the organic solvent, typically via evaporation, ultimately, resulting in a lipid film. The lipid film is hydrated with an aqueous media to form liposomes. The nanoliposomes produced can be run through an extruder in order to make sure the final sample of liposomes has a relatively uniform size distribution. The disadvantages to this method are that they sometimes produce multilamellar vesicles, which limit their entrapment abilities for siRNA (Maherani et al. 2011).

Another technique is the Heating Method developed by Mozafari. This method produces nanoliposomes by hydrating the phospholipid components in an aqueous solution of 3% glycerol and increasing the temperature to 60°C. The glycerol increases the stability of the vesicles and prevents coagulation. This method allows for large-scale manufacture of the liposomes in one step without employing toxic solvents or detergents (Mozafari. 2010).

The microfluidization method is a method of production that avoids using toxic solvents. This method is based on the principle of dividing a pressure stream of about 10,000 psi into two parts, passing through a small opening and directing the flows of steam at each other. The shear and impact forces reduces the particle sizes of the liposomes. A large volume of nanoliposomes can be produced with this technique. Additionally, the nanoliposomes are not exposed to detergents or organic solvents (Mozafari. 2010).

There are two main techniques to capture siRNA in nanoliposomes, passive trapping and active trapping. Passive trapping involves entrapment during the nanoliposome formation process, and active trapping involves loading the siRNA into already formed nanoliposomes. Passive trapping relies on the fact that nanoliposomes capture a certain aqueous volume, including any solutes, during formation. The efficacy of this encapsulation technique depends on the phospholipid concentrations, lamellarity, and morphology of the nanoliposomes. The active trapping technique involves empty nanoliposomes in a concentrated siRNA solution, and disrupting the nanoliposomes temporarily so that the drugs can enter the nanoliposomes. In both cases, the siRNA-nanoliposomes must be purified to remove any free siRNA before analyzing the samples (Maherani et al. 2011).

1.10 Nanoliposome Characterization Techniques

Nanoliposomes must be characterized after fabrication to ensure that they met the intended specifications. There are several separate methods that are used to characterize size, lamellarity, encapsulation efficiency, and to visualize the nanoliposomes.

Maintaining a constant size over time is important for stability characterization. Dynamic light scattering is a widely used technique to characterize size of nanoliposomes. Dynamic light scattering, however, does not provide information regarding the shape of the nanoliposomes. It also assumes that the aggregation of more than one liposome is a single particle (Maherani et al. 2011).

Entrapment efficiency can be difficult to measure, as siRNA can be trapped in one of the layers of the nanoliposome, adsorbed on the nanoliposome surface, or encapsulated in the inner region of the nanoliposome. Some current methods used are UV/VIS Spectrometry, FCS, and spectrofluorimetry (Maherani et al. 2011). However, one of the most common methods to measure siRNA-encapsulation, however, is the RiboGreen Assay. The RiboGreen Assay requires that the nanoliposomes must be destroyed, so that the encapsulated siRNA can float freely, and the RiboGreen dye can bind to the siRNA. The fluorescence of the samples is measured using fluorescence fluctuation spectroscopy.

Lamellarity is a more difficult characteristic to detect. Microscopically observation can provide a visualization of the nanoliposome, but the conditions under which the sample must be prepared may alter the structure of the nanoliposome. Additionally, lamellarity of nanoliposomes can be detected using, “P-nuclear magnetic resonance to monitor the signal intensity of the phospholipid phosphorus at the outer monolayer compared to the total signal” (Maherani et al. 2011).

The TCSPC system in our lab allows us to identify the size, encapsulation efficiency, and diffusion characteristics of nanoliposomes simultaneously instead of running several individual assays. This ultimately saves time, cost, and efficiency in a laboratory setting.

The radius is obtained from FCS data for nanoliposomes by using the 3D diffusion equation, $r^2 = 6D\tau_D$, solving for D, where r=0.4233E-6 m, the radius of the confocal volume, and τ_D is obtained from the FCS curve fitting. The value for D is used to solve for R by rearranging the Stokes Einstein equation, $R = \frac{k_b T}{6\pi\eta D}$, where k_b=1.38E-23 J/K, T is the temperature at which the experiment is run, and η=0.001 Pa·s, the viscosity of water.

Chapter 2

Materials and Methods

2.1 siRNA-Nanoliposome Fabrication

Nanoliposomes are fabricated by developing a film of a specific lipid formulation in a round-bottom flask, followed by hydrating the film, and finally, by extruding the solution through an Avanti extrusion device. The nanoliposomes used to encapsulate siRNA were made from a 47.5/47.5/5 DOPE/DOTAP/DOPS-PEG molar ratio formulation (Buyens et al. 2009).

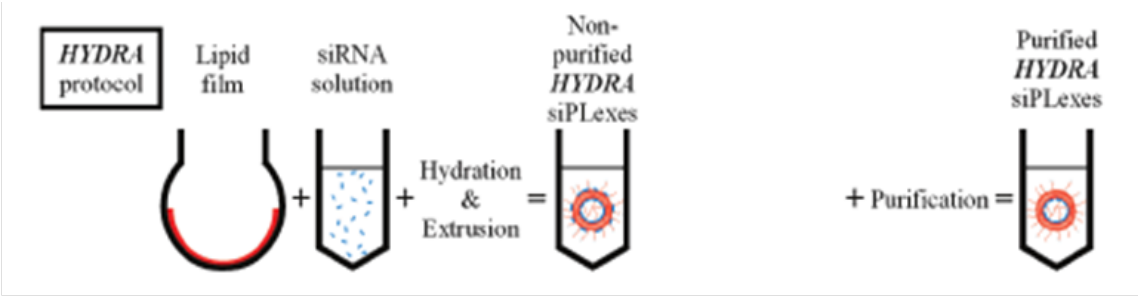

Figure 2.1.1 Schematic of HYRDRA siRNA-Nanoliposome Preparation (Buyens et al. 2009)

The lipid mixture is placed in a round-bottom flask. The chloroform is evaporated from the lipid solution using an inert gas, argon. Following the evaporation process, the round-bottom flask is placed in a vacuum chamber to ensure that all of the chloroform has evaporated from the lipid film. Once the a round-bottom flask was removed from the vacuum chamber, 1.1 ml of a 2 nM Avanti Alex-Flour tagged siRNA in Hepes Buffer (10 μM) solution was added to the round-bottom flask to begin the hydration process. Alex-Flour tagged siRNA excites at a wavelength 555 nm.

A stopper was placed in a round-bottom flask to minimize evaporation, and then the flask was placed on a heating block at 60°C. Every five minutes, the round-bottom flask is removed from the heating block and vortexed gently. After 40 minutes, the extrusion process begins. The

nanoliposomes pushed through the Avanti Polar Lipids Extrusion kit 21 times. The extrusion kit contains filters that attempt to create uniform 100 nm nanoliposomes (Buyens et al. 2009).

After the extrusion process, the siRNA-nanoliposomes must be purified to eliminate free-floating siRNA. GE PD-10 desalting columns were used in this purification process. The first purification stem removed the free siRNA. Seven samples were collected from the column. Samples 3-5 were found to be free of free-floating siRNA. Following this step, RNAse was used to remove siRNA located on the external surface of the siRNA. Samples 3-5, following their exposure to RNAse, were run through the PD-10 desalting columns to remove the nucleotide remnants of the siRNA.

2.2 **Nanoliposome Fabrication**

Nanoliposomes were made from 47.5/47.5/5 DOPE/DOTAP/DOPS-PEG molar ratio formulation (Buyens et al. 2009) and encapsulated DiI to test the stability and properties of the formulation to be used to encapsulate siRNA. The protocol discussed in Section 2.1 is the same protocol used for the formulation of the 47.5/47.5/5 DOPE/DOTAP/DOPS-PEG without the siRNA.

2.3 **TCSPC Set-Up**

Figure 2.3 below showcases the optical set up of the system in our laboratory. The pulsed laser beam is transmitted by fiber coupled to the confocal port. The beam is collimated with lens L1, and expanded by lenses L2 and L3. Mirrors M1 and M2 direct the beam so that it can reflect off of the dichroic mirror DM1. The beam enters the right port of the microscope (Gullapalli et al. 2007).

The fluorescence emission signal from the excitation of the sample is collimated by the objective and passes through the side port, passing through the dichroic mirror. Lens L4 focuses

the signal and it moves through the optical fiber that is connected to the photomultiplier tube (PMT). The PMTs convert single photons to electrical pulses. These pulses are then directed to the TCSPC board (Gullapalli et al. 2007).

Laser light from the TIRF system is part of the back port of the microscope along with the epifluorescence tube (Epi). Lenses L5 and L6 collimate the epifluorescence and TIRF light, respectively. Lens L7 focuses the TIRF light on the objective back aperture. When the sliding mirror is moved from the light path, the right side port is closed and the emission signal can be collected by the camera by the tube lens (TL). Though epifluorescence and TIRF are not utilized in our studies of siRNA-nanoliposomes, they are very important components of the system in our laboratory and showcase the multifaceted abilities of this system (Gullapalli et al. 2007).

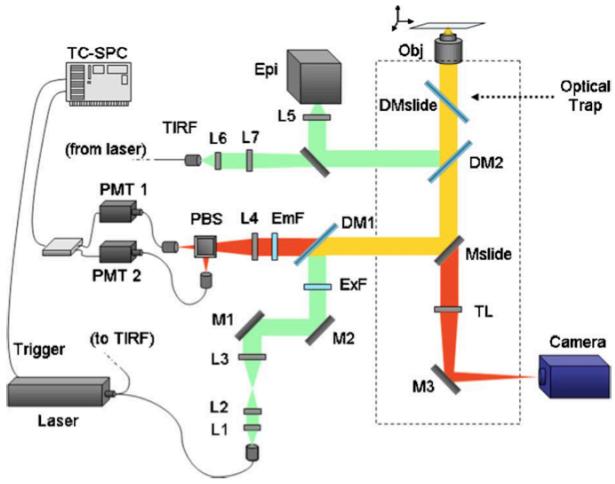

Figure 2.3 Set-up of TCSPS System in our laboratory (Gullapalli et al. 2007)

2.4 TCSPC Protocol

The cooler is turned on to cool the laser system. Once the cooler has run for 15 minutes and is ready to use, the laser controller is turned on, and the laser key is turned into the "on" position. The cap where the objective goes is removed, and the laser power is checked. It should

be between 40-80 μW. The objective is fixed on the microscope with coverslip correction collar set at 0.17. The focus knob is turned all the way down and approximately 12 μL of water is placed on the objective. A glass coverslip is placed over the objective and the focus knob is turned up until the coverslip comes in contact with the objective. 200 μL of the sample is placed on the coverslip and the DCC module is turned on. The SPCM software is loaded and the outputs are enabled on the DCC module. Oscilloscope measurements are taken first, and then FIFO measurements are taken and saved to undergo further analysis of the FCS curves.

2.5 Nanoliposome Analysis from FCS Data

The autocorrelation curves from FCS were fit using equation 4 using a Levenberg – Marquardt nonlinear least-squares regression algorithm using Origin software. The quality of the curve fits was examined by minimizing residuals. Values for τ_D, the number of molecules in the confocal volume and N are obtained from this curve fit. The photon count for the sample can be obtained from the raw data files (Gullapalli et al. 2007).

Dynamic light scattering is also performed using a Viscotek 802 DLS model on the nanoliposomes that encapsulated DiI, as well as the siRNA-nanoliposomes to verify the size of the nanoliposomes.

2.6 Measuring Encapsulation Efficiency

The encapsulation efficiency can be measured by comparing the molecular brightness data from the siRNA-nanoliposomes to the molecular brightness of a single siRNA particle. The following equations are used to calculate the encapsulation efficiency:

$$MB = \frac{Photon\ Count}{Number\ of\ molecules\ in\ confocal\ volume\ (N)} \quad (6)$$

$$\#\ of\ siRNA\ per\ nanoliposome = \frac{MB_{nanoliposome}}{Average\ MB_{siRNA}} \quad (7)$$

However, these calculations do not illustrate whether the siRNA is encapsulated in the nanoliposome, or bound to the exterior of the liposome. It is the hope that the use of RNAses followed by the use of the desalting columns removes the siRNA bound to the exterior of the nanoliposomes.

Chapter 3

Results

3.1 Nanoliposome Stability Results

Four samples of DOPE/DOTAP/DOPS-PEG nanoliposomes that encapsulated DiI were analyzed at three different points over the course of 16 days to determine the stability of this nanoliposome formulation. The results are for τ_d can be seen in Figure 3.1.1 below with standard deviation error bars. The results for R can be seen in Figure 3.1.2 with standard deviation error bars. The average results for each day of each sample are summarized in Table 3.1.1. The FCS curves from which these values were derived from can be seen in Appendix A. The DLS figures used to verify the sizing of the nanoliposomes can be seen in Appendix C.

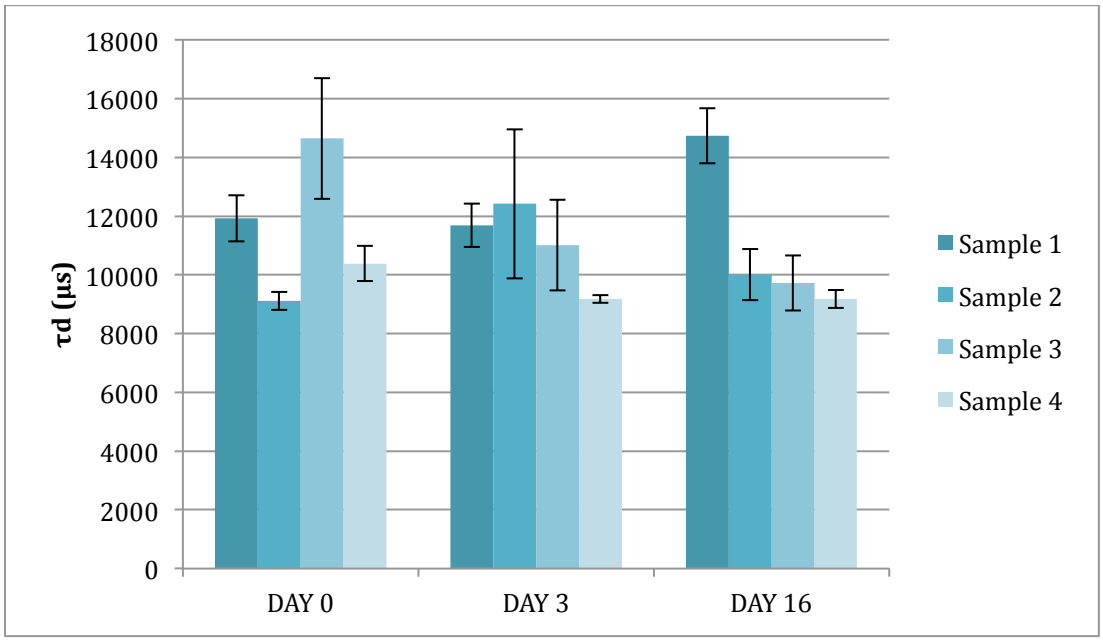

Figure 3.1.1 τ_d values for four DOPE/DOTAP/DOPS-PEG nanoliposome samples tested over the course of 16 days.

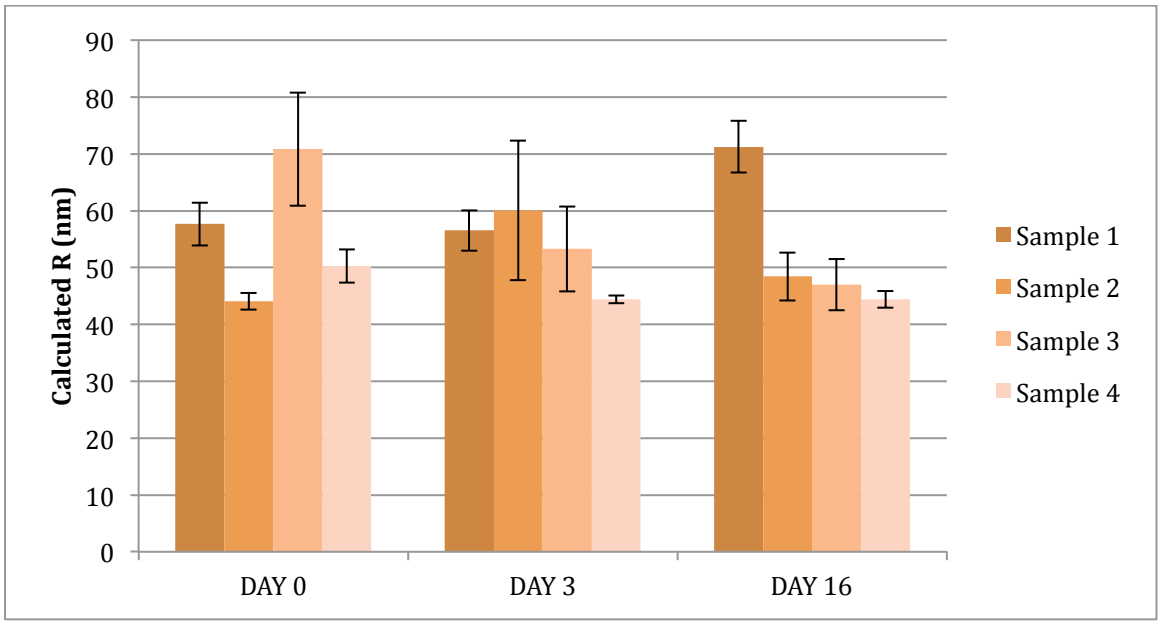

Figure 3.1.2 Radius (nm) values for four DOPE/DOTAP/DOPS-PEG samples tested over the course of 16 days.

Table 3.1.1 Comparison of average τd and R values for all four samples over the course of 16 days

	Day 0		Day 3		Day 16	
	τd (μs)	R (nm)	τd (μs)	R (nm)	τd (μs)	R (nm)
Sample 1	11,922.96	57.68	11,683.62	56.52	14,731.26	71.26
Sample 2	9,111.99	44.08	12,419.99	60.08	10,009.87	48.42
Sample 3	14,645	70.85	11,013	53.28	9,718.75	47.02
Sample 4	10,388	50.25	9,178	44.40	9,176	44.39

3.2 Molecular Brightness measurements of siRNA-Nanoliposomes

Before the molecular brightness of siRNA-nanoliposomes could be determined, the molecular brightness of the siRNA had to be determined. The results can be seen in Figure 3.2.1. The standard value of the molecular brightness of siRNA was taken to be the average of all of

these obtained values, 1,650 counts/second. The raw data for the molecular brightness measurements can be seen in Appendix B.

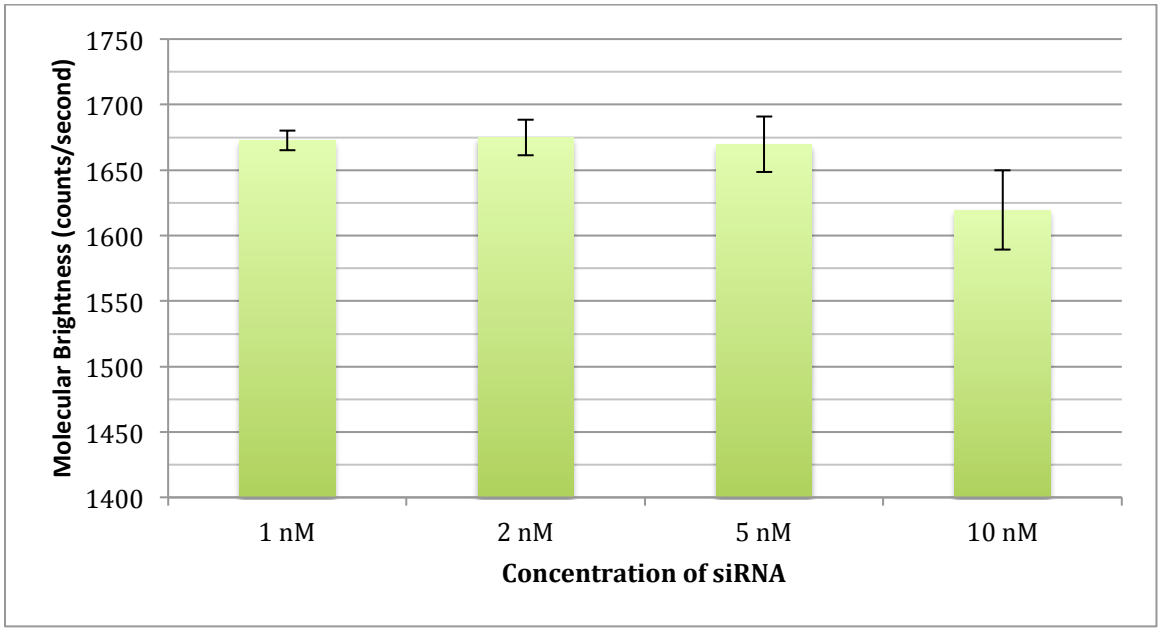

Figure 3.2.1 Molecular Brightness of varying concentrations of Alexa-Flour tagged siRNA

3.3 Encapsulation Efficiency Results

The intensity of the fluorescence of the siRNA-nanoliposomes was so great with each trial that even with very dilute samples the FCS data could not be curve fit with our algorithm because the DCC, the detector controller card, frequently reset during each trial. The DCC provides for power supply, gain control, and overload shutdown. There are no counts obtained at a low DCC gain, at a specific DCC gain, count rates rise steeply, and when the gain is too high, the DCC shuts down and resets (Becker. 2008). The multichannel tracer curves (MCS) from each trial were analyzed to get an approximation of how many siRNA were encapsulated in each nanoliposome. One of the MCS curves used to analyze the siRNA-nanoliposomes can be seen in Figure 3.3.1. A histogram of the number of siRNA encapsulated in the nanoliposomes can be seen in Figure 3.3.2. This histogram was compiled from the data of all of MCS curves, which can be seen in Appendix D.

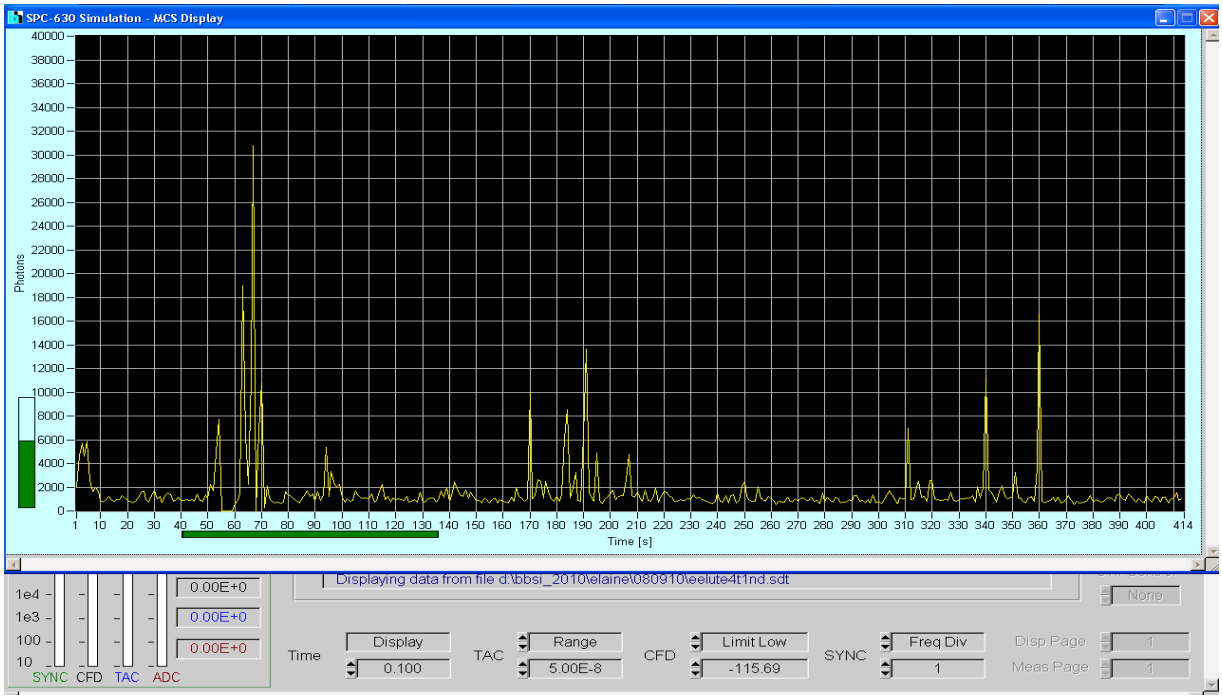

Figure 3.3.1 MCS curve for siRNA-nanoliposomes

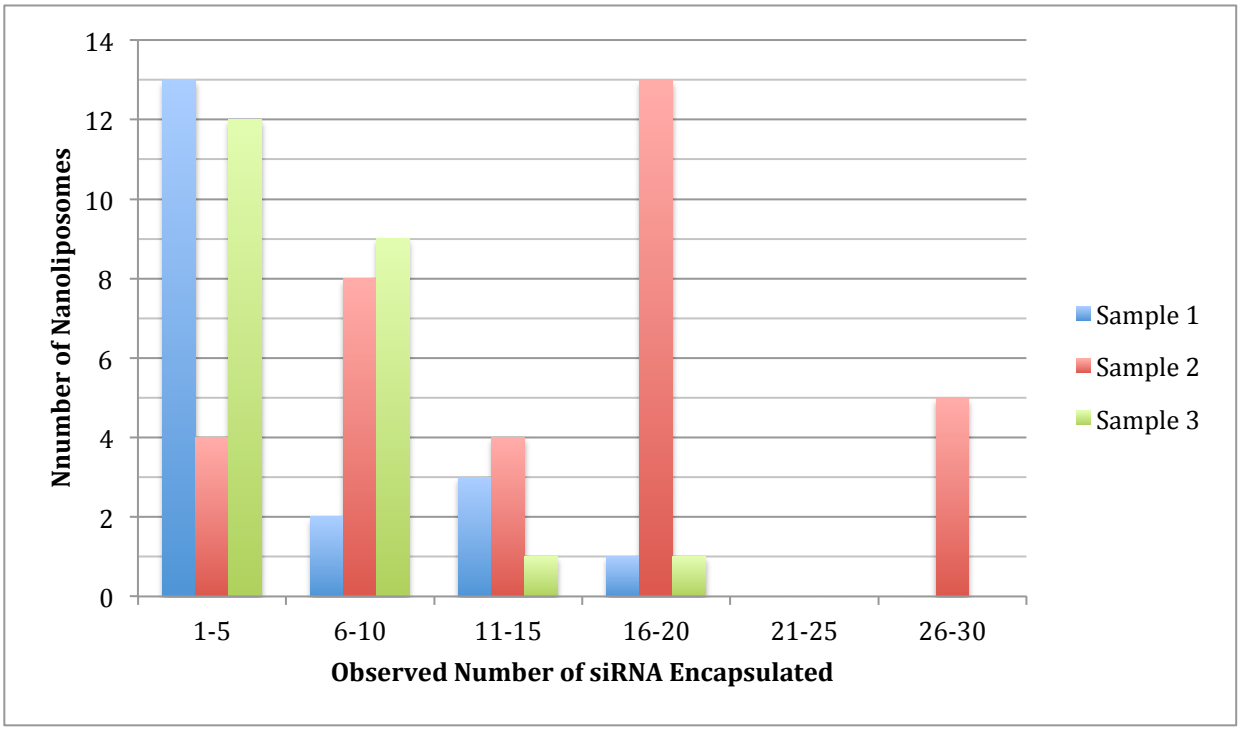

Figure 3.3.2 Histogram of encapsulated siRNA in nanoliposomes

3.4 Discussion and Conclusions

The DOPE/DOTAP/DOPS-PEG nanoliposome samples are relatively stable over the course of the tested 16 day period. The radii results do not show fragmentation as determined from the FCS and DLS data. The radii are also the size that was intended to be produced, approximately 50 nm. The diffusion time is relatively consistent for all samples over the course of the 16 days, showing that this nanoliposome formulation is stable, and that each sample possesses similar diffusion characteristics. Our TCSPC system is ideal to analyze nanoliposome sizes due to the fact that we can obtain size, diffusion time, and encapsulation efficiency data all from one trial, whereas DLS, the most commonly used sizing technique, can only provide details regarding the sizes of the nanoliposomes.

Though the FCS data could not be curve fitted, the MCS curves provide an estimate of how many siRNA are encapsulated per nanoliposome. As seen in Figure 3.3.2, there is an inconsistent number of siRNA molecules encapsulated in each nanoliposome. The majority of the nanoliposomes had 1-5 siRNA molecules encapsulated, and very few had more than 26 siRNA molecules encapsulated. These low siRNA encapsulation numbers could be attributed to the fact that the concentration of the Alex-Flour siRNA that was used in the HYDRA method was 2 nM, as to avoid resetting the DCC during FCS trials. Perhaps, in future testing this concentration should be greater, in hopes to encapsulate more siRNA. Additionally, further research must be done in order to refine the formulation method to encapsulate a more consistent number of siRNA molecules per nanoliposome.

This study has shown that siRNA can be encapsulated into DOPE/DOTAP/DOPS-PEG nanoliposomes, and that TCSPC system in our laboratory is effective to determine many properties of these siRNA-nanoliposomes simultaneously. While we were not able to curve fit the FCS data, it was clear that there were siRNA molecules in these samples, and that the number of siRNA per nanoliposome could be quantified without destroying the nanoliposomes. Unlike

the RiboGreen assay, the fluorescence of all of the siRNA molecules present in these samples can be seen in FCS. With the RiboGreen assay, there is no way to be certain that all of the nanoliposomes have been destroyed, and all of the siRNA present in these samples is accessible to the RiboGreen dye. Additionally, there is no way to quantify how many siRNA molecules were encapsulated in each individual nanoliposome, and only an average number of siRNA molecules per nanoliposome can be obtained. It is clear that no other lab techniques currently used to analyze siRNA-nanoliposomes on a single vesicle basis, are like our TSCPC system that can provide all of this data on one system.

Very recently, a neutral density filter was added to the TCSPC system in our laboratory. Now that this filter is in place, we may be able to run FCS more effectively and obtain data from curve fits of the siRNA-nanoliposomes without having to rely on the MCS curves. This neutral density filter reduces the intensity of the scattered light, and would hopefully avoid the DCC resetting.

Furthermore, though the nanoliposomes were stable over a 16 day period, the long-term stability of these vesicles should be assessed. This time period was helpful to study these nanoliposomes in the laboratory. However, for any clinical use, these nanoliposomes should have a longer shelf-life than 16 days. A shelf-life of approximately one year would be helpful in order to make this therapeutic option as cost effective as possible (Schroeder et al. 2009). Therefore, one larger batch could be produced and many patients could be treated from this one production.

The number of siRNA per nanoliposome should be analyzed to determine if there is a way to encapsulate a similar number of siRNA in each liposome. Additionally, the number of nanoliposomes that did not encapsulate any siRNA molecules should be analyzed. Though, this may be very difficult to test, this information would be helpful in determining the overall efficiency of the siRNA-nanoliposome production.

An additional area of study for these siRNA-nanoliposomes would be to vary the concentrations of cationic lipids to determine the effect on siRNA encapsulation. This would hopefully provide information regarding the ideal concentration of DOTAP to encapsulate the most siRNA effectively.

Once the siRNA-nanoliposome encapsulation efficiency has been maximized, it would be interesting to add ligands for cell-surface receptors to the siRNA-nanoliposomes to target specific cell types *in vitro*. This testing would showcase the pharmaceutical efficacy of these siRNA-nanoliposomes. However, adding cell-surface integrins to the siRNA-nanoliposomes may affect the encapsulation efficiency of the siRNA, and this will have to be thoroughly analyzed as studies advance in this area.

Appendix A

Florescence Correlation Spectroscopy Figures

The figures below are the FCS curves for the nanoliposomes that encapsulated DiI. FCS was performed over a 16-day period. The information from these figures can be seen in Figure 3.3.1 and 3.3.2.

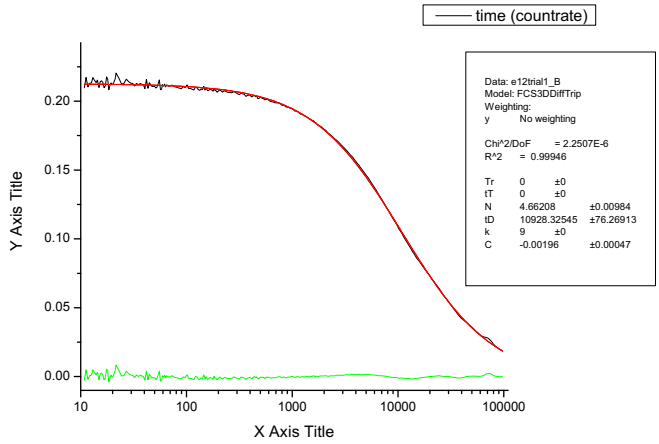

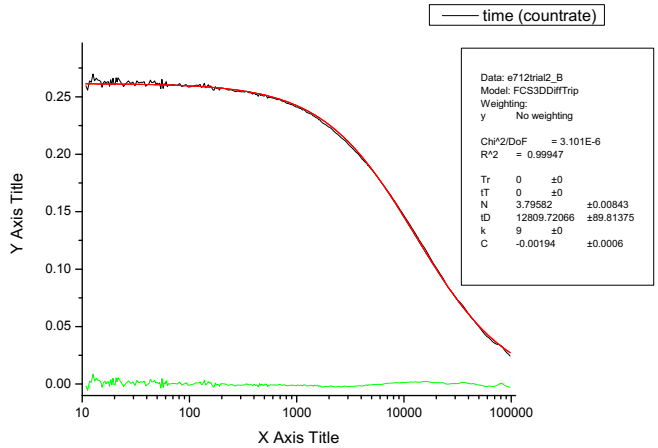

Figure A.1 FCS Plots for Sample 1 at Day 0

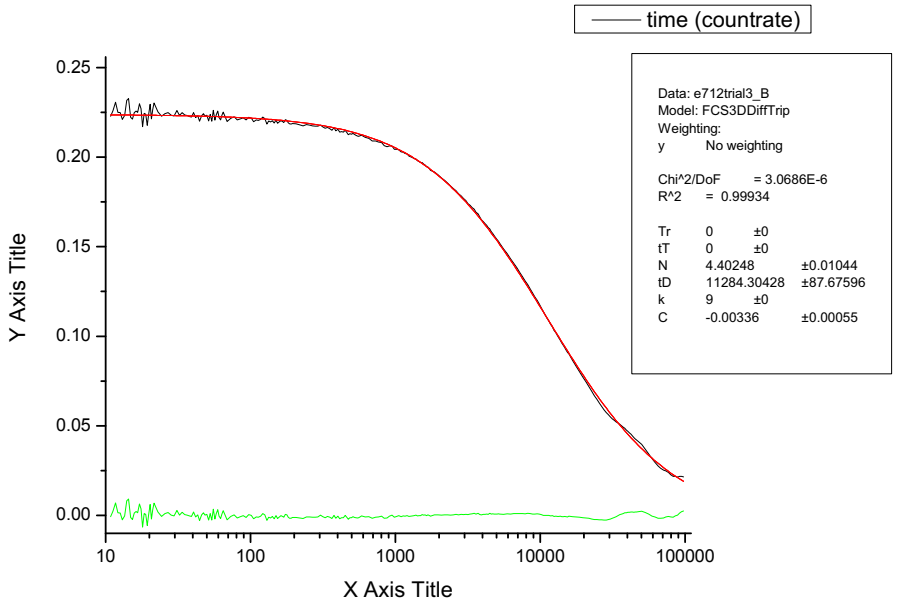

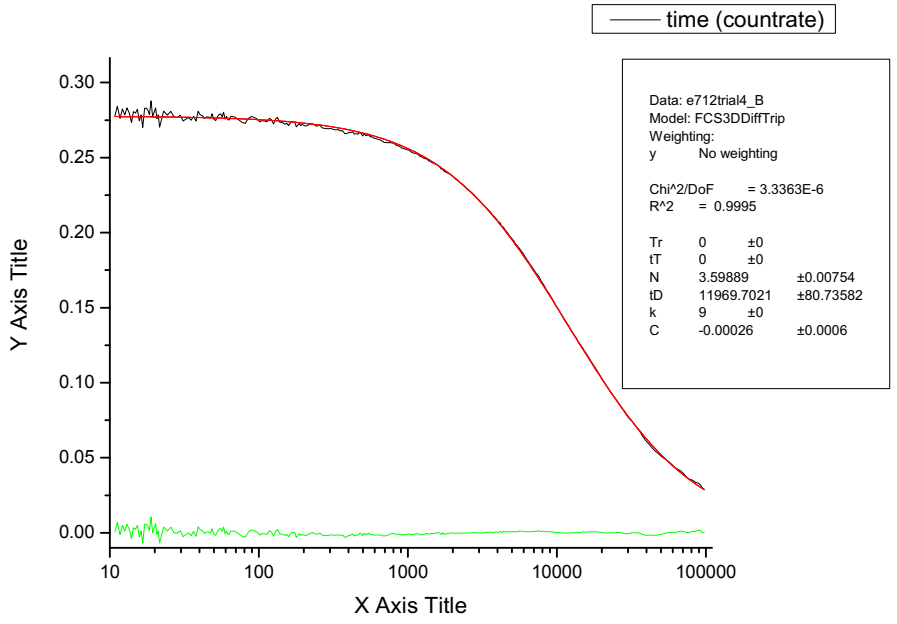

Figure A.2 FCS Plots for Sample 2 at Day 0

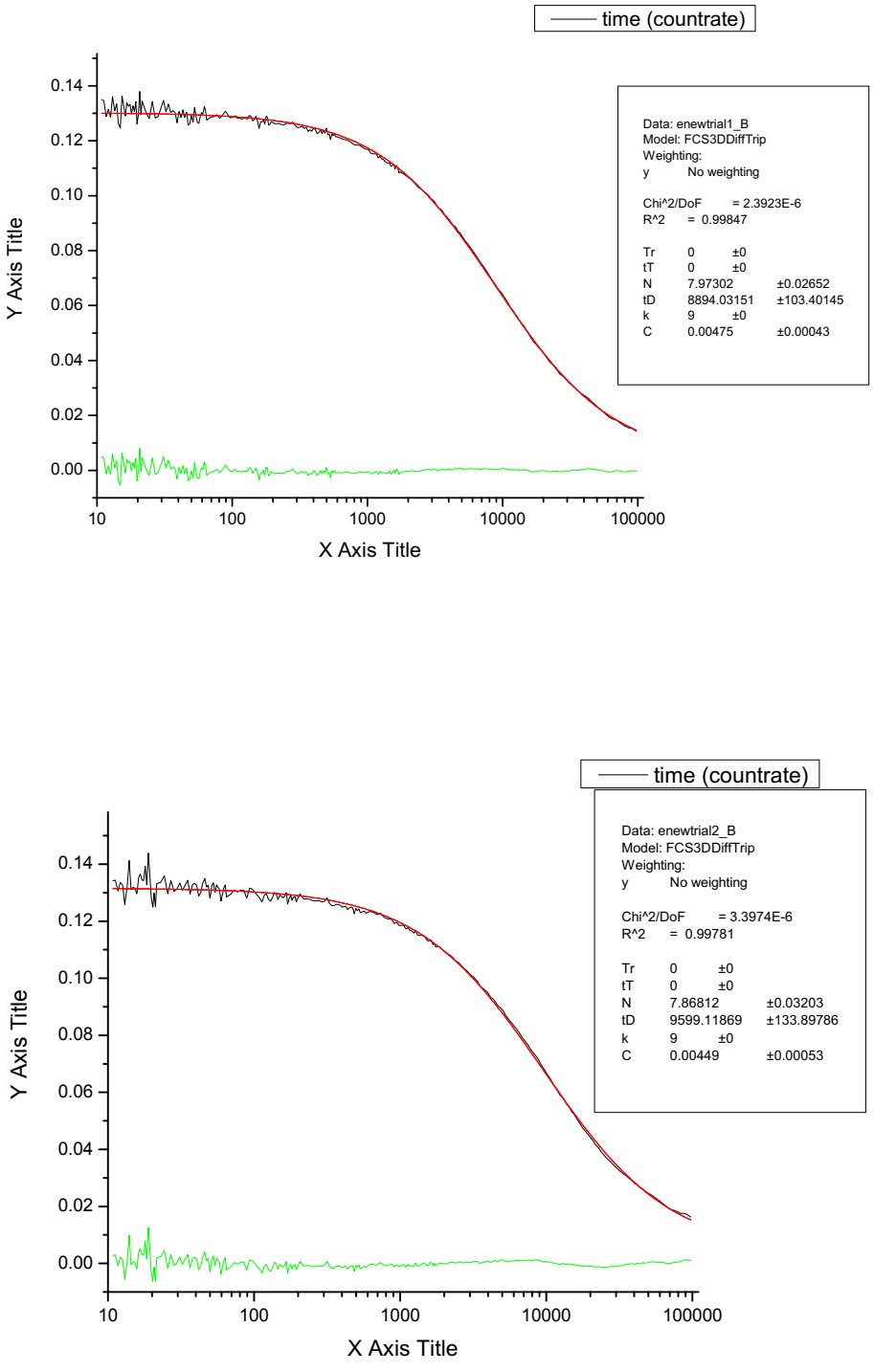

Figure A.3 FCS Plots for Sample 3 at Day 0

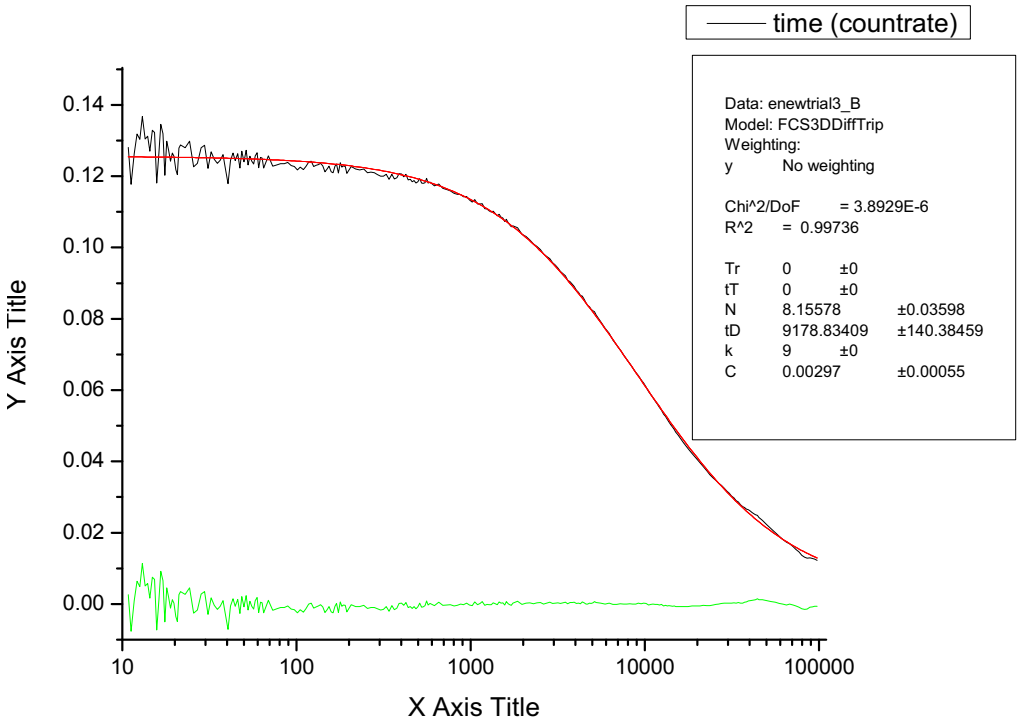

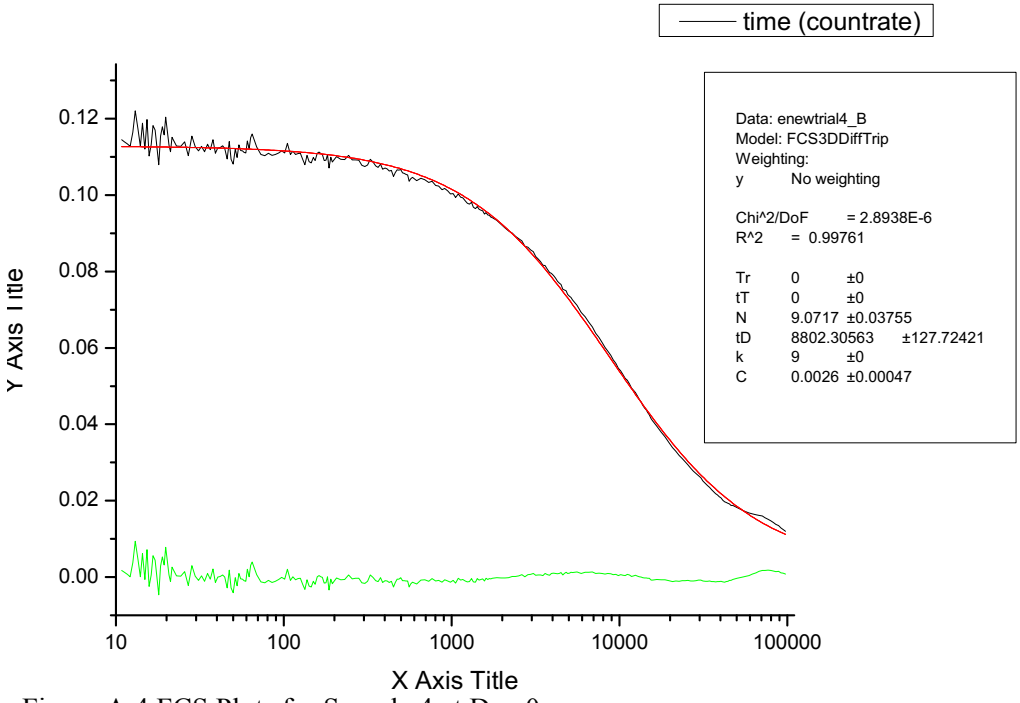

Figure A.4 FCS Plots for Sample 4 at Day 0

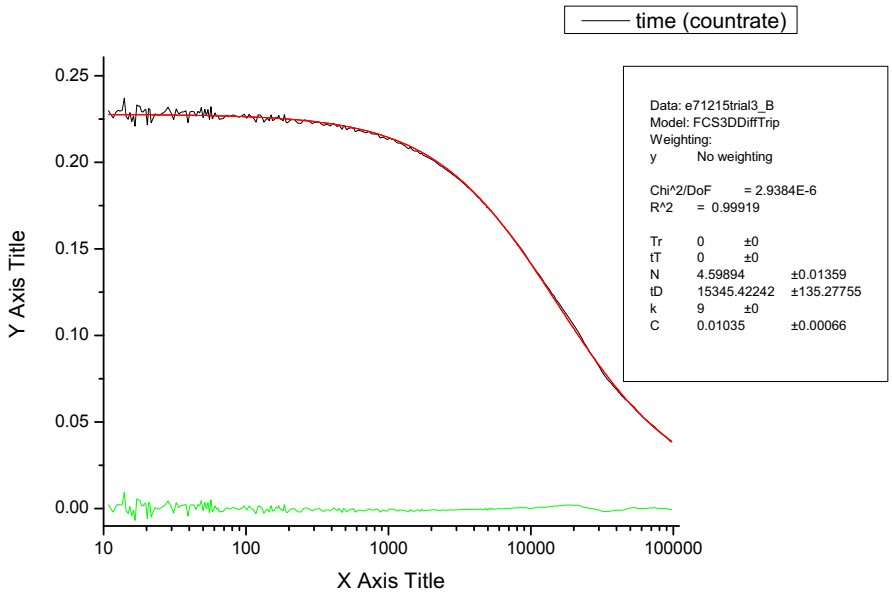

Figure A.5 FCS Plot for Sample 1 at Day 3

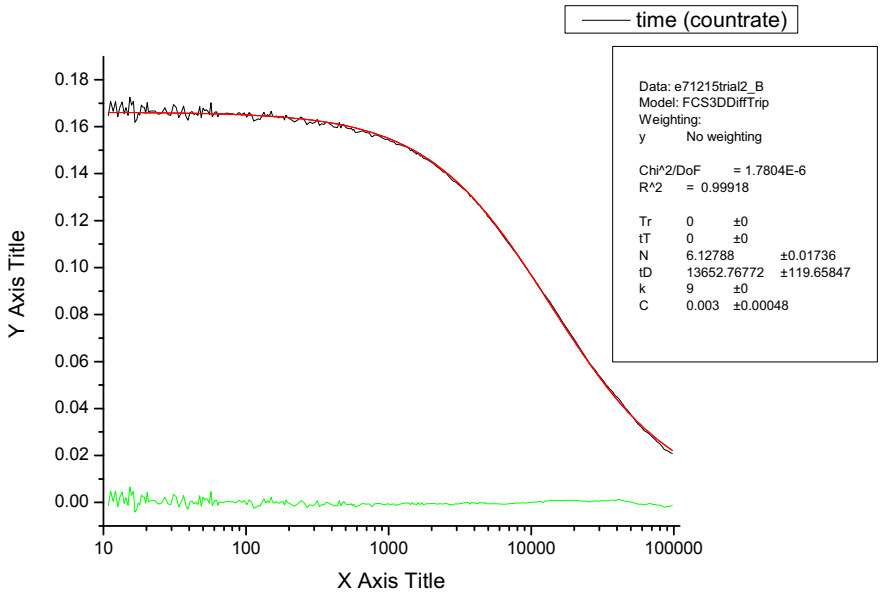

Figure A.6 FCS Plot for Sample 2 at Day 3

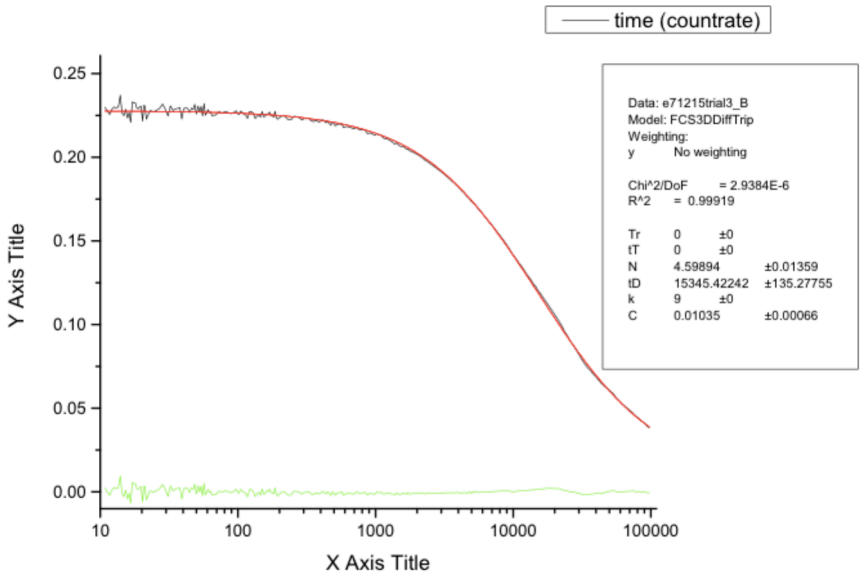

Figure A.7 FCS Plot for Sample 3 at Day 3

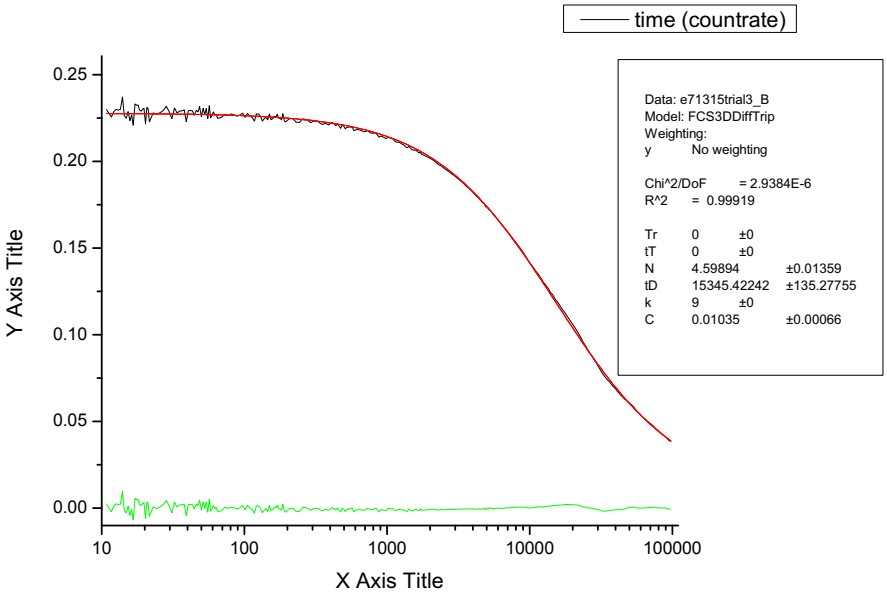

Figure A.8 FCS Plot for Sample 4 at Day 3

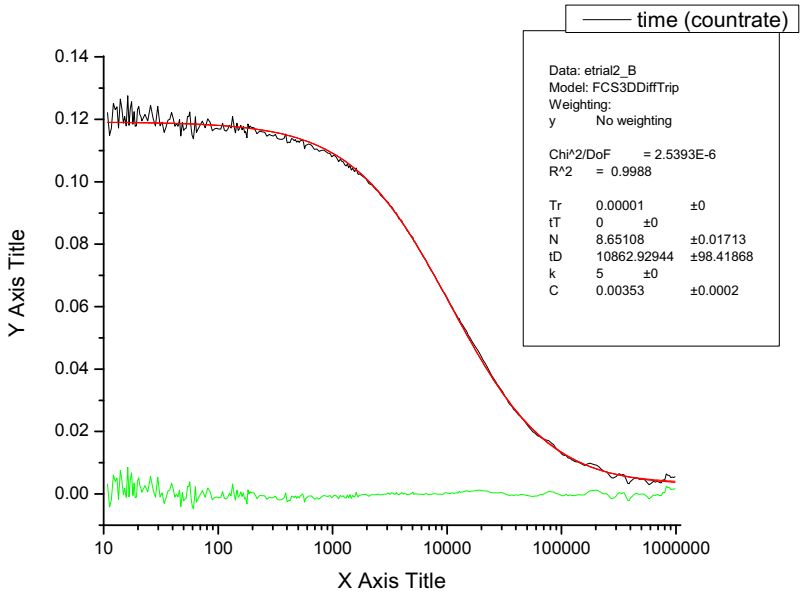

Figure A.9 FCS Plot for Sample 1 at Day 16

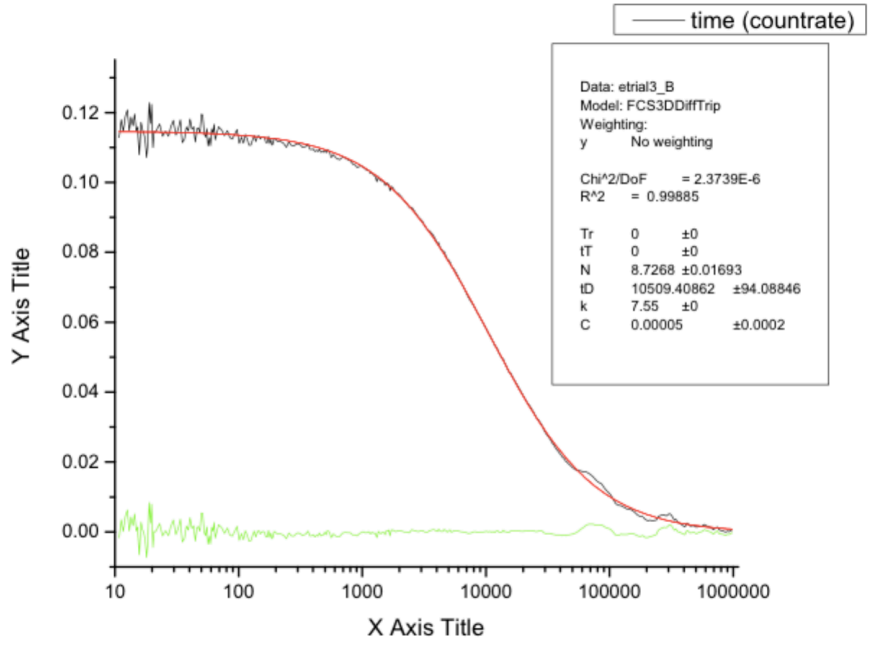

Figure A.10 FCS Plot for Sample 2 at Day 16

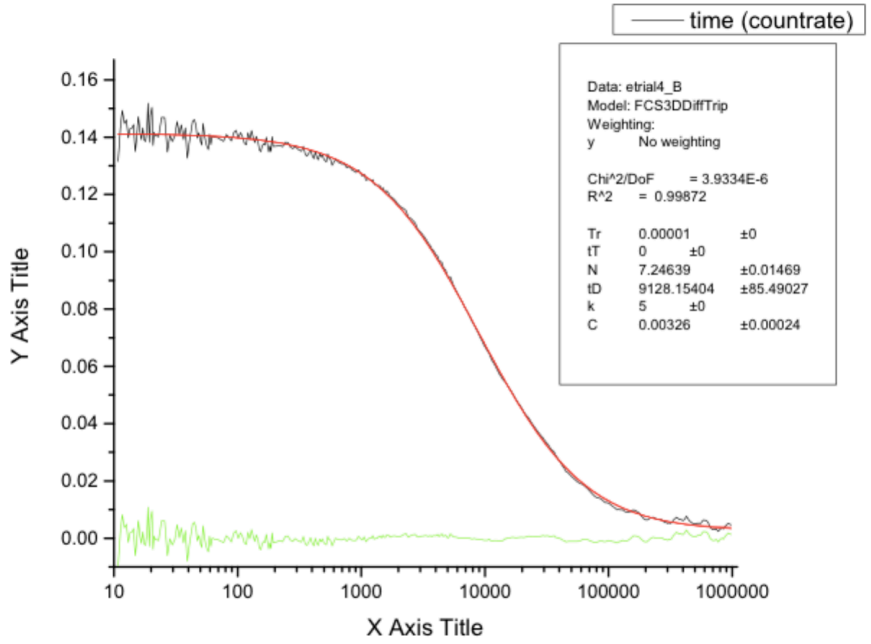

Figure A.11 FCS Plot for Sample 3 at Day 16

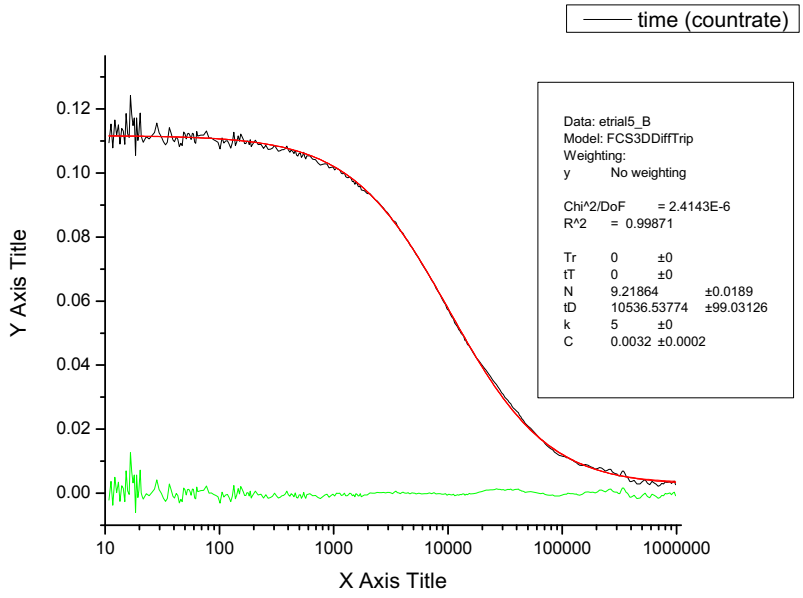

Figure A.12 FCS Plot for Sample 4 at Day 16

Appendix B

siRNA Molecular Brightness Data

Table B.1 Raw data from Alex-Flour tagged siRNA properties derived from FCS

Attempted Concentration (nM)	τd (μs)	N	D (μm^2/s)	Calculated R (nm)	Photon Count	Molecular Brightness
1	519.06	6.93	86.30	2.51	11,607.00	1,674.89
1	508.89	6.74	88.02	2.46	11,329.00	1,680.86
1	520.37	5.65	86.08	2.52	9,269.00	1,640.53
1	527.21	5.98	84.97	2.55	10,135.00	1,694.82
2	510.78	13.563	87.70	2.47	22,085.00	1,628.33
2	537.42	13.502	83.35	2.60	22,562.00	1,671.01
2	507.49	14.625	88.27	2.46	24,758.00	1,692.85
2	521.85	13.61	85.84	2.52	23,236.00	1,707.27
5	551.62	33.05	81.21	2.67	53,444.00	1,617.07
5	501.36	33.55	89.35	2.43	56,295.00	1,677.94
5	519.15	32.91	86.29	2.51	55,756.00	1,694.20
5	515.21	29.89	86.95	2.49	50,522.00	1,690.26
10	499.35	64.198	89.71	2.42	100,856.04	1,571.02
10	560.36	61.402	79.94	2.71	101,171.24	1,647.69
10	502.138	62.305	89.21	2.43	102,746.00	1,649.08
10	505.812	58.974	88.56	2.45	98,736.00	1,674.23
10	489.04	54.431	91.60	2.37	98,076.30	1,801.85
10	512.75	61.8	87.36	2.48	95,275.00	1,541.67
10	567.61	64.61	78.92	2.75	102,497.00	1,586.40
10	506.91	64.45	88.37	2.45	100,440.00	1,558.42
10	556.38	65.8	80.51	2.69	101,691.00	1,545.46
						AVERAGE
						1,649.80

Appendix C

DLS Figures for Nanoliposomes

The DLS figures below were used to verify the FCS results for the stability of nanoliposomes over a 16 day period. These results closely matched the radii derived from the FCS data for these samples.

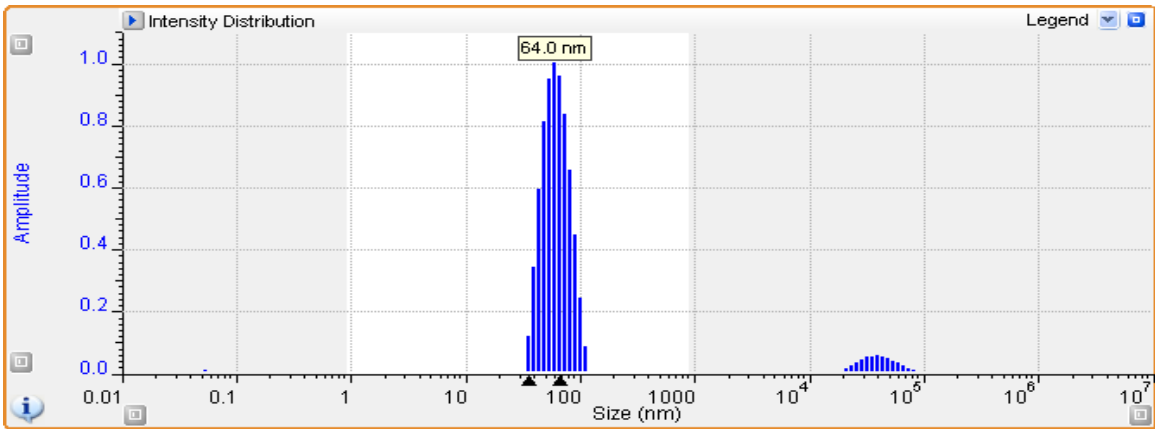

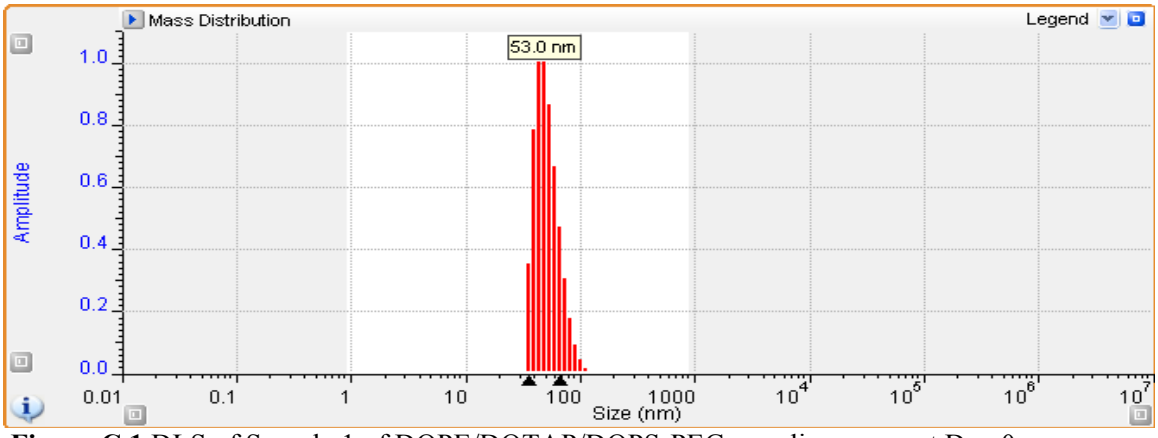

Figure C.1 DLS of Sample 1 of DOPE/DOTAP/DOPS-PEG nanoliposomes at Day 0

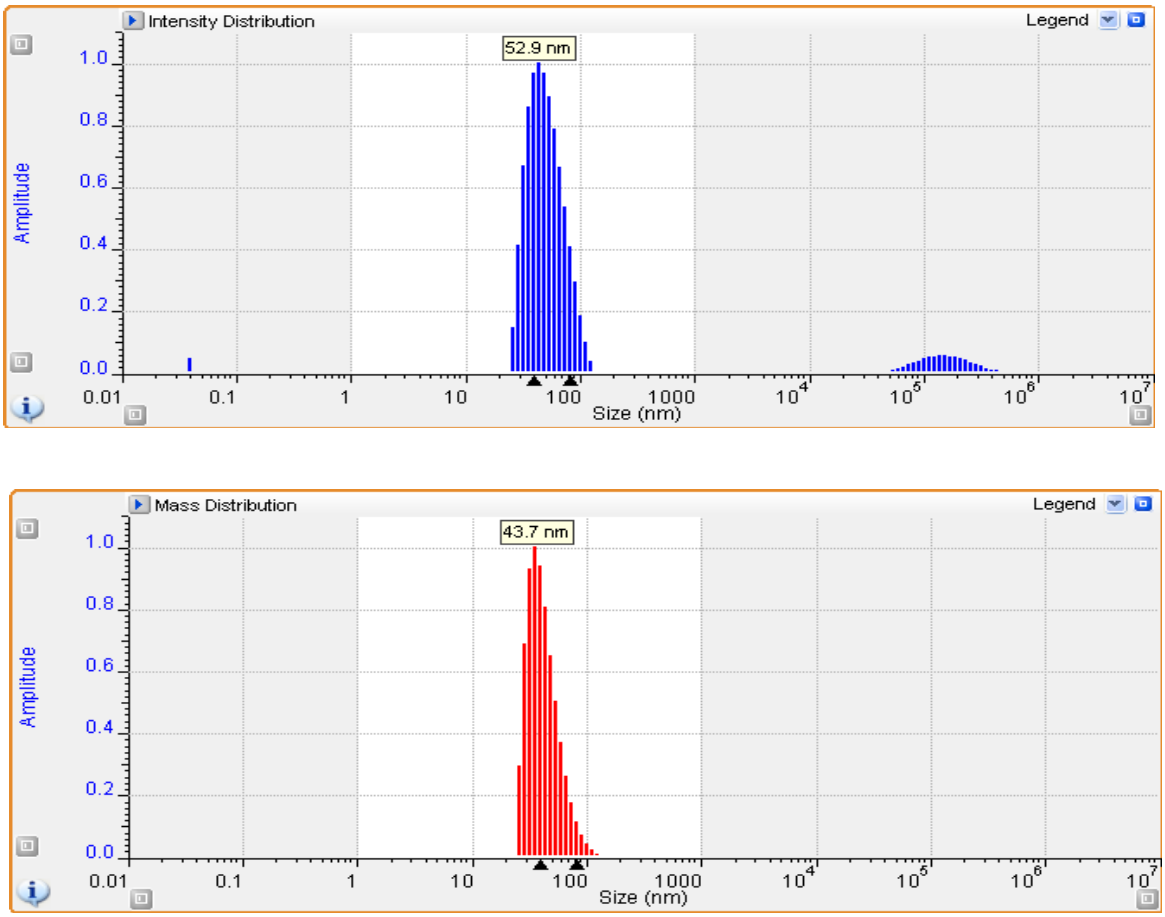

Figure C.2: DLS of Sample 1 DOPE/DOTAP/DOPS-PEG nanoliposomes at Day 16

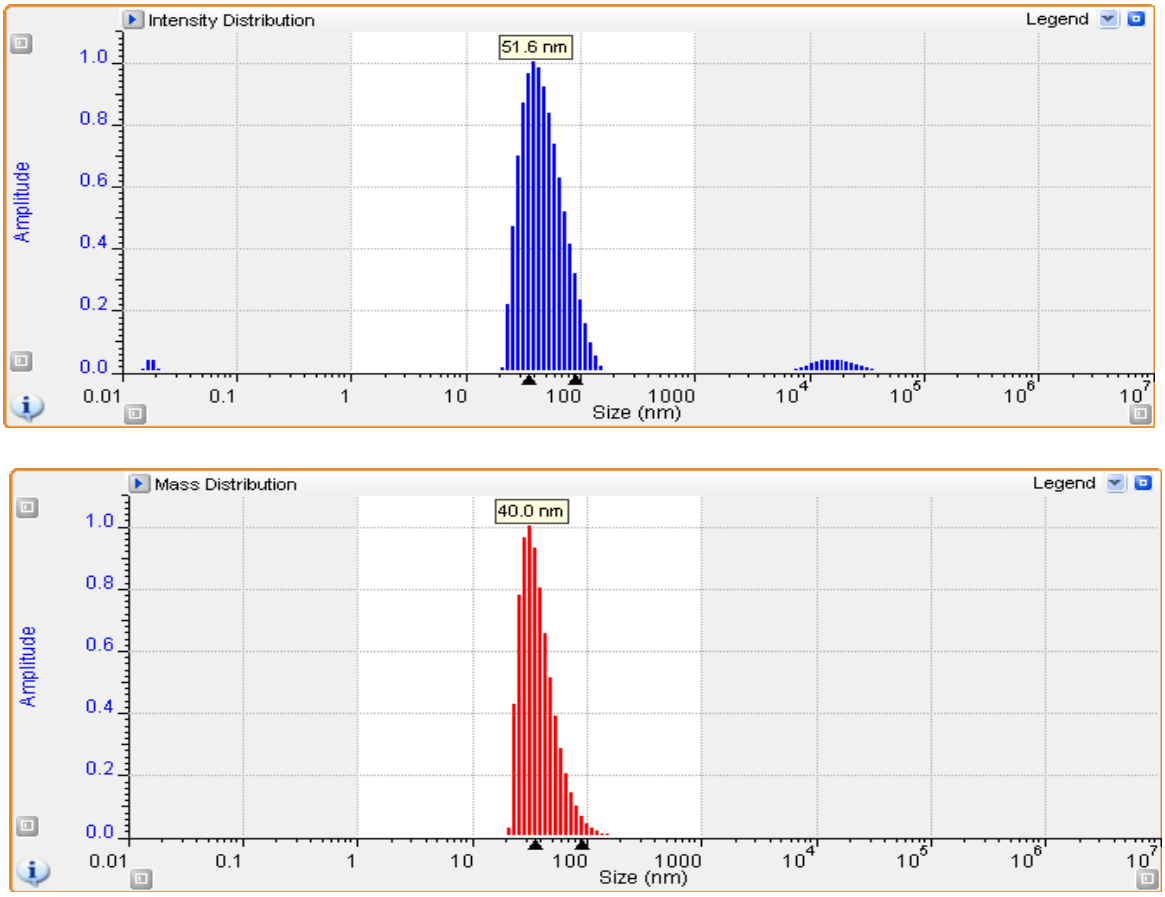

Figure C.3: DLS of Sample 2 DOPE/DOTAP/DOPS-PEG nanoliposomes at Day 0

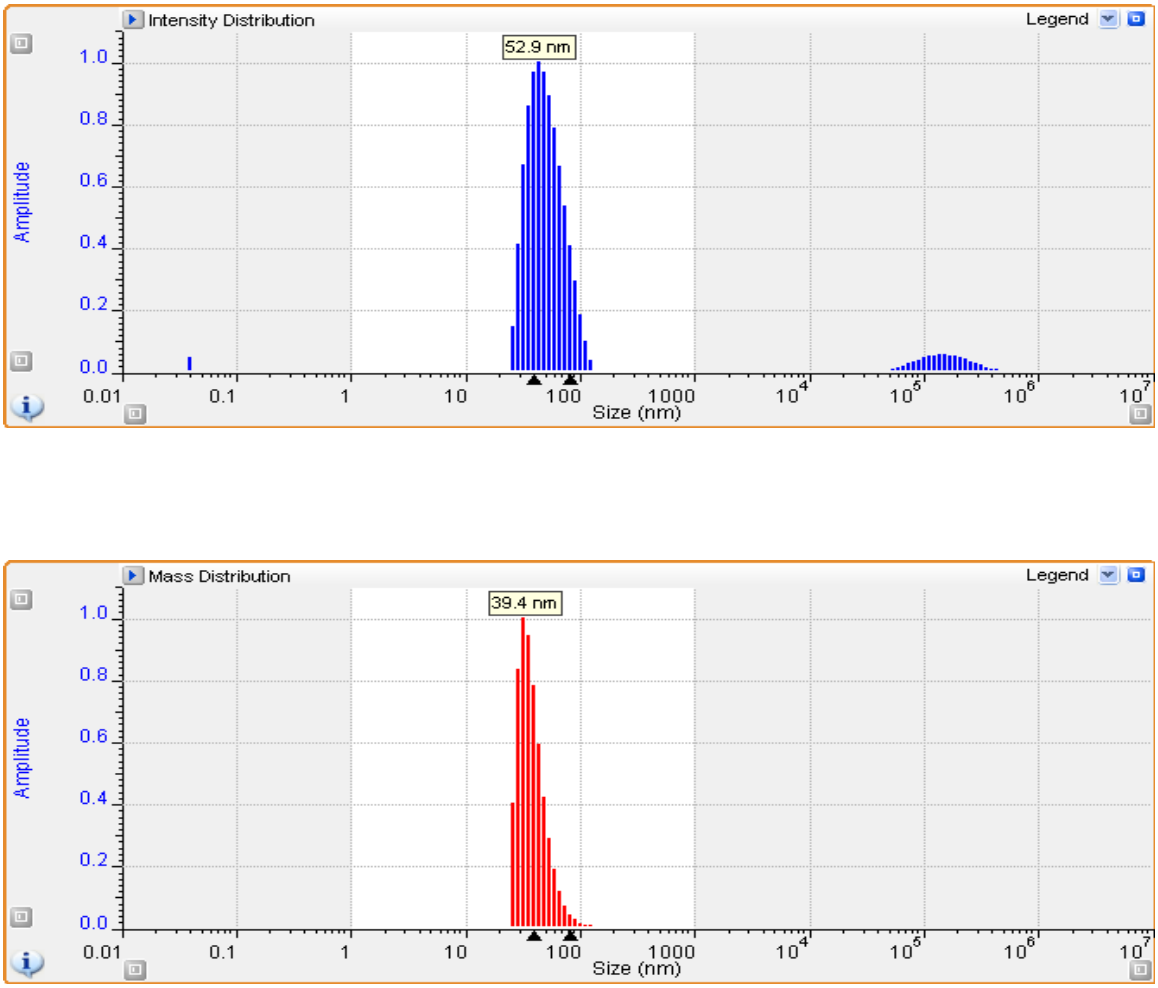

Figure C.4: DLS of Sample 2 DOPE/DOTAP/DOPS-PEG nanoliposomes at Day 16

Appendix D

siRNA-nanoliposome MCS Curves

These MCS curves were used to determine how many siRNA molecules were encapsulated in each nanoliposome. The magnitude of the peaks present in each MCS curve is divided by the molecular brightness of one siRNA molecule to determine how many siRNA molecules are encapsulated in a nanoliposome.

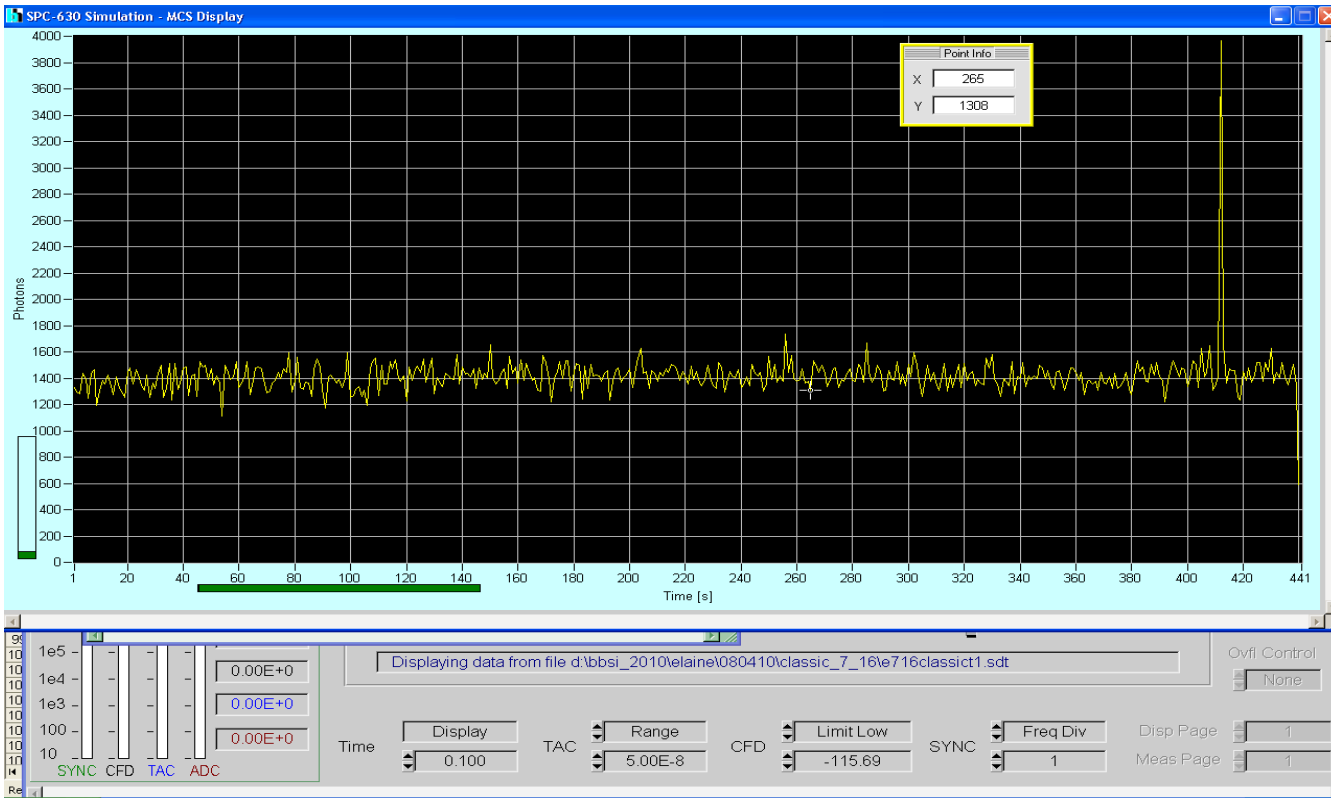

Figure D.1 MCS for siRNA-nanoliposomes sample 1, trial 1

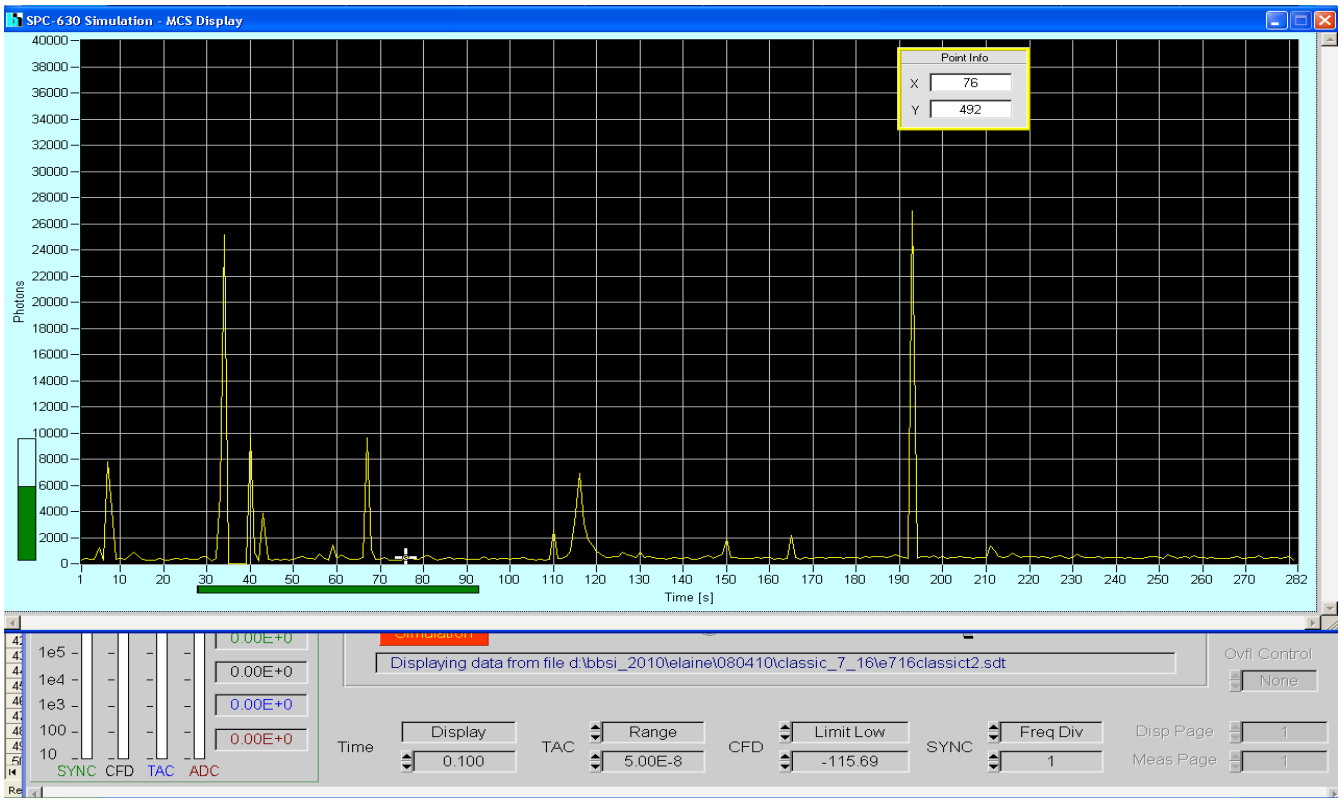

Figure D.2 MCS for siRNA-nanoliposomes sample 1, trial 2

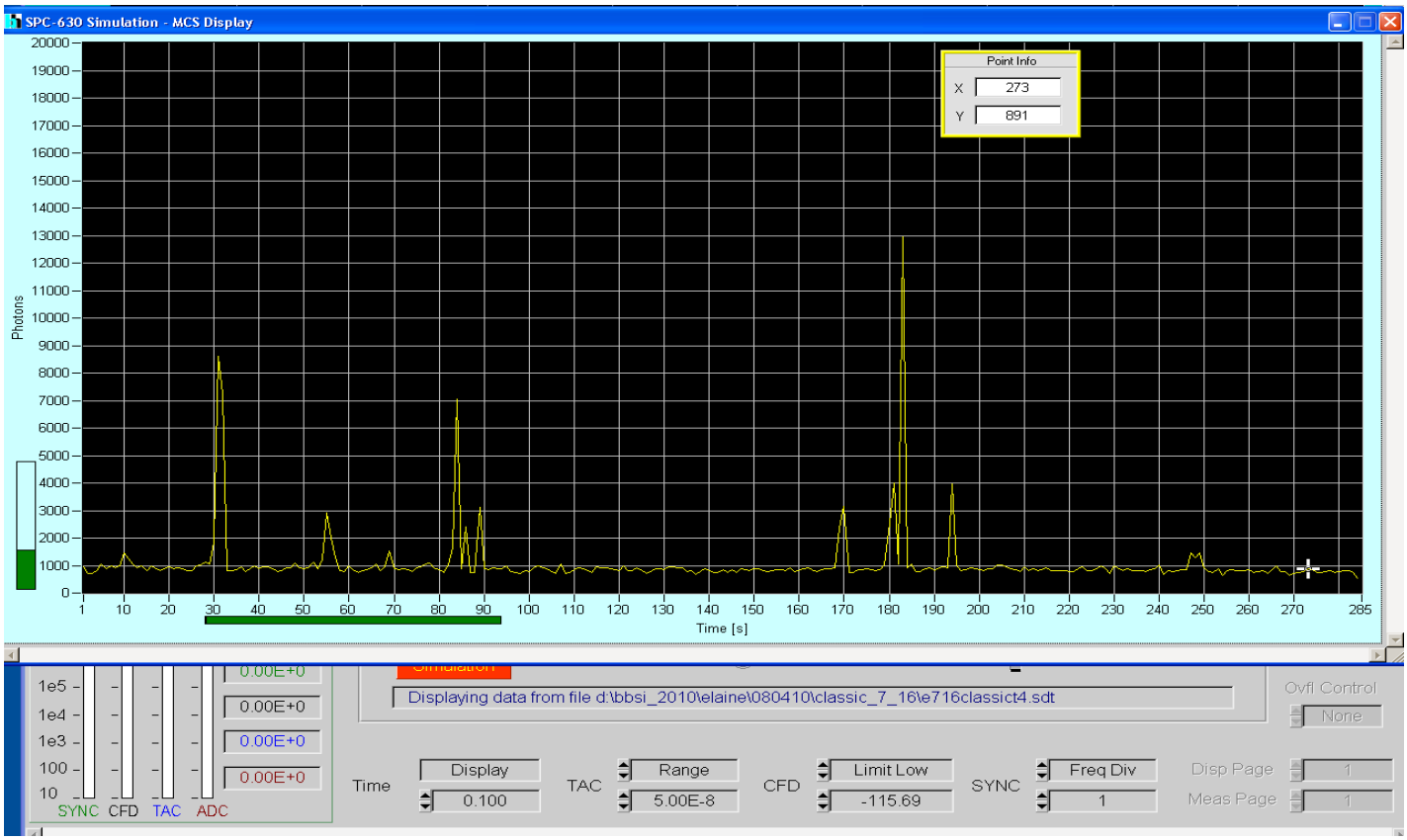

Figure D.3 MCS for siRNA-nanoliposomes sample 1, trial 3

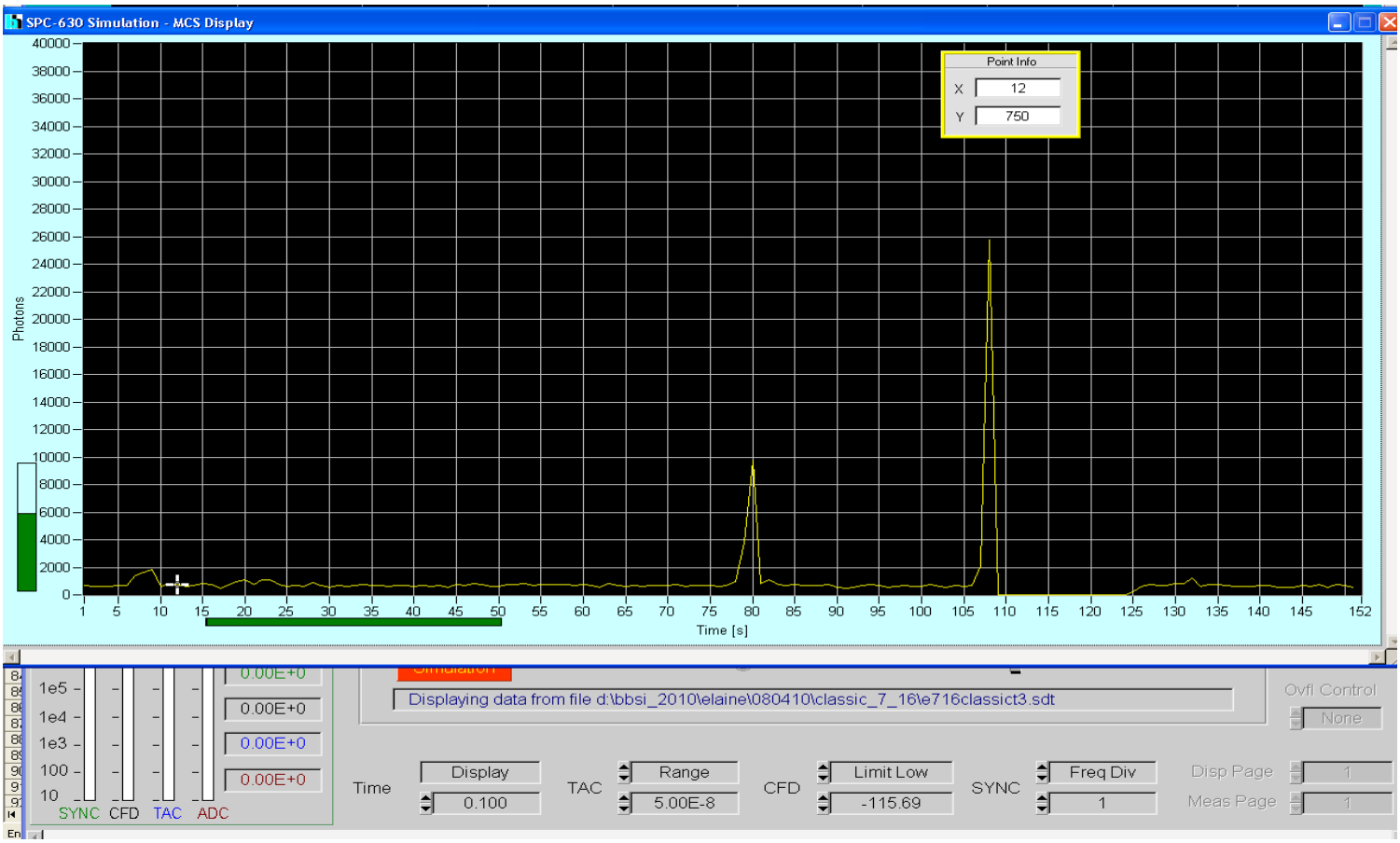

Figure D.4 MCS for siRNA-nanoliposomes sample 1, trial 4

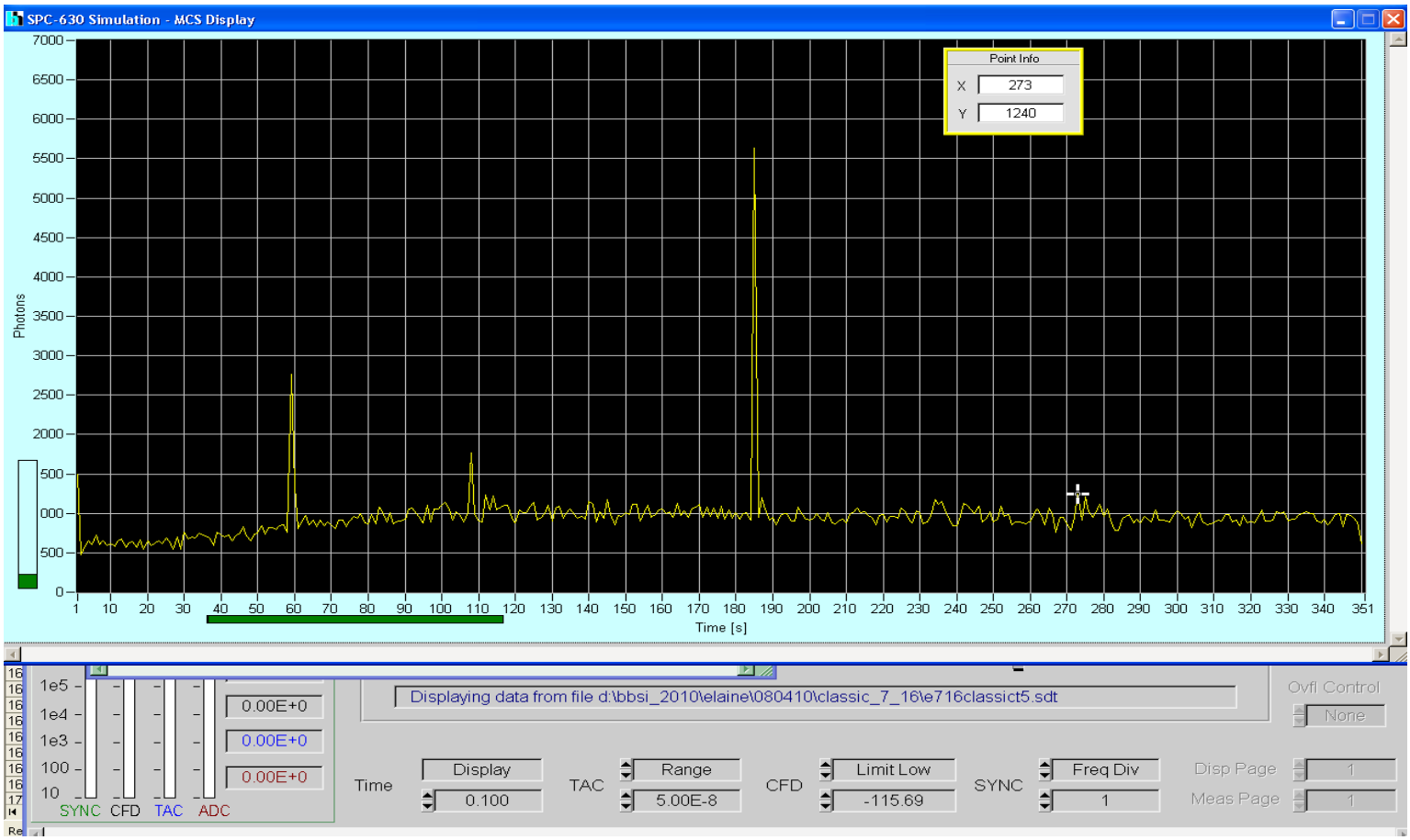

Figure D.5 MCS for siRNA-nanoliposomes sample 1, trial 5

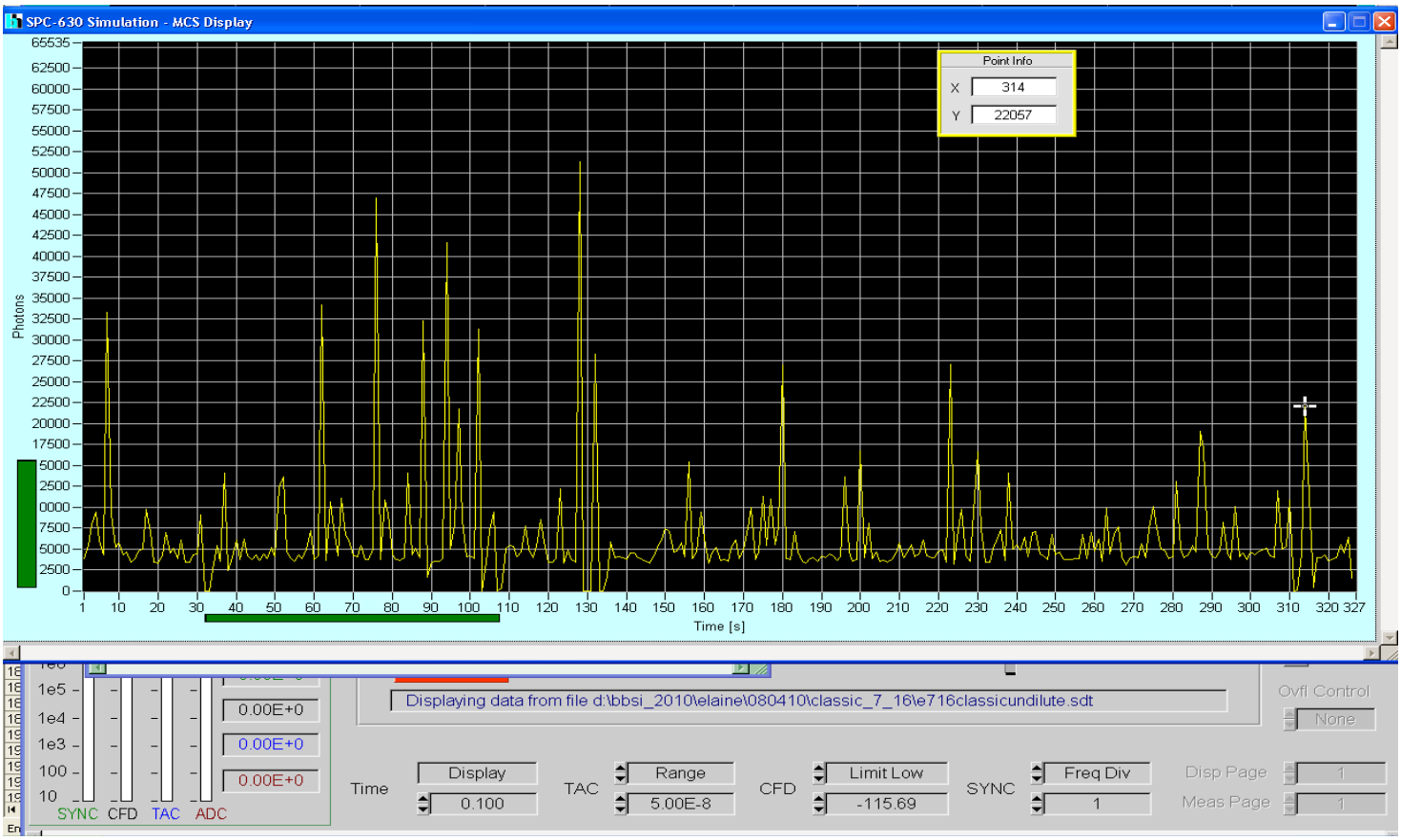

Figure D.6 MCS for siRNA-nanoliposomes sample 2, trial 1

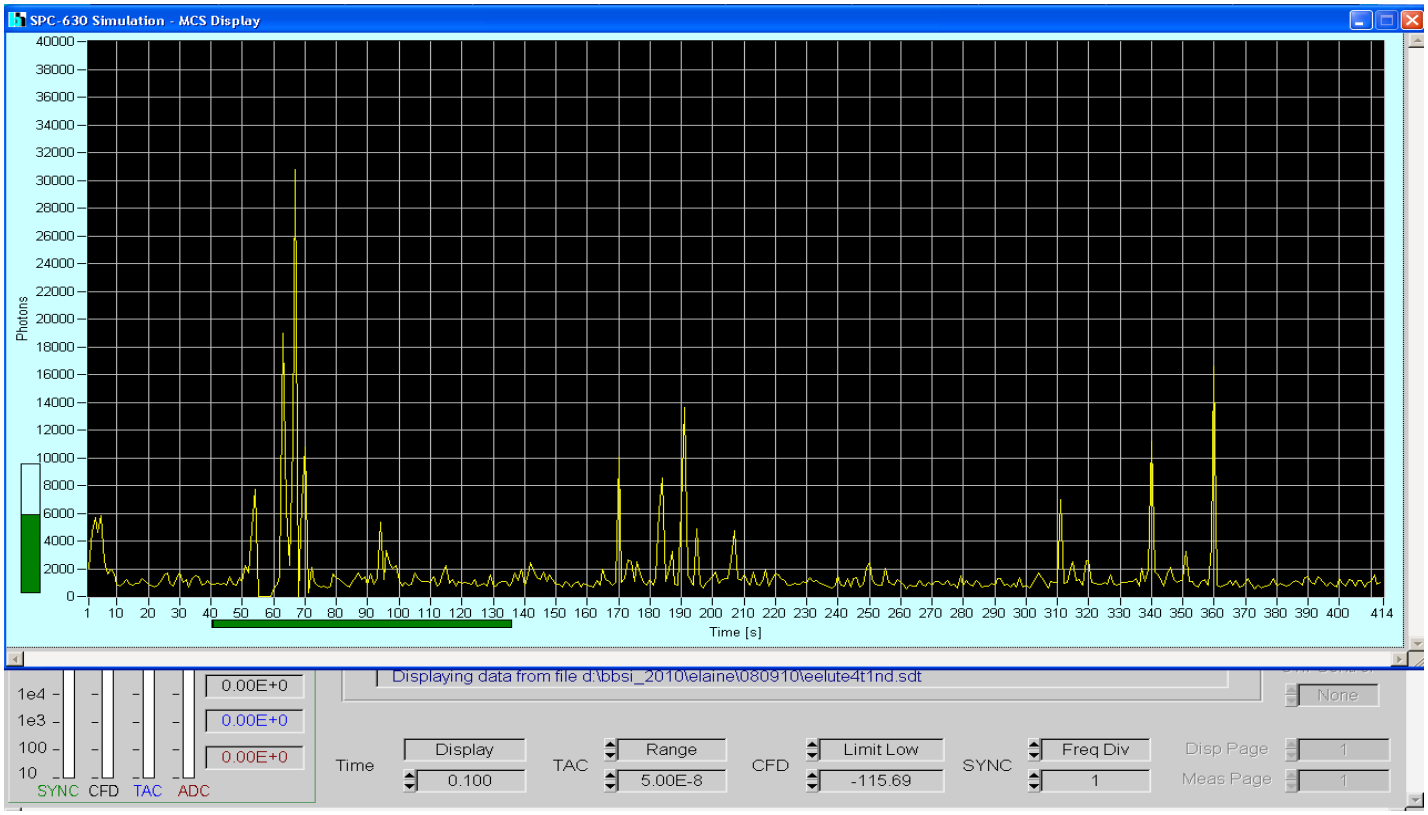

Figure D.7 MCS for siRNA-nanoliposomes sample 2, trial 3

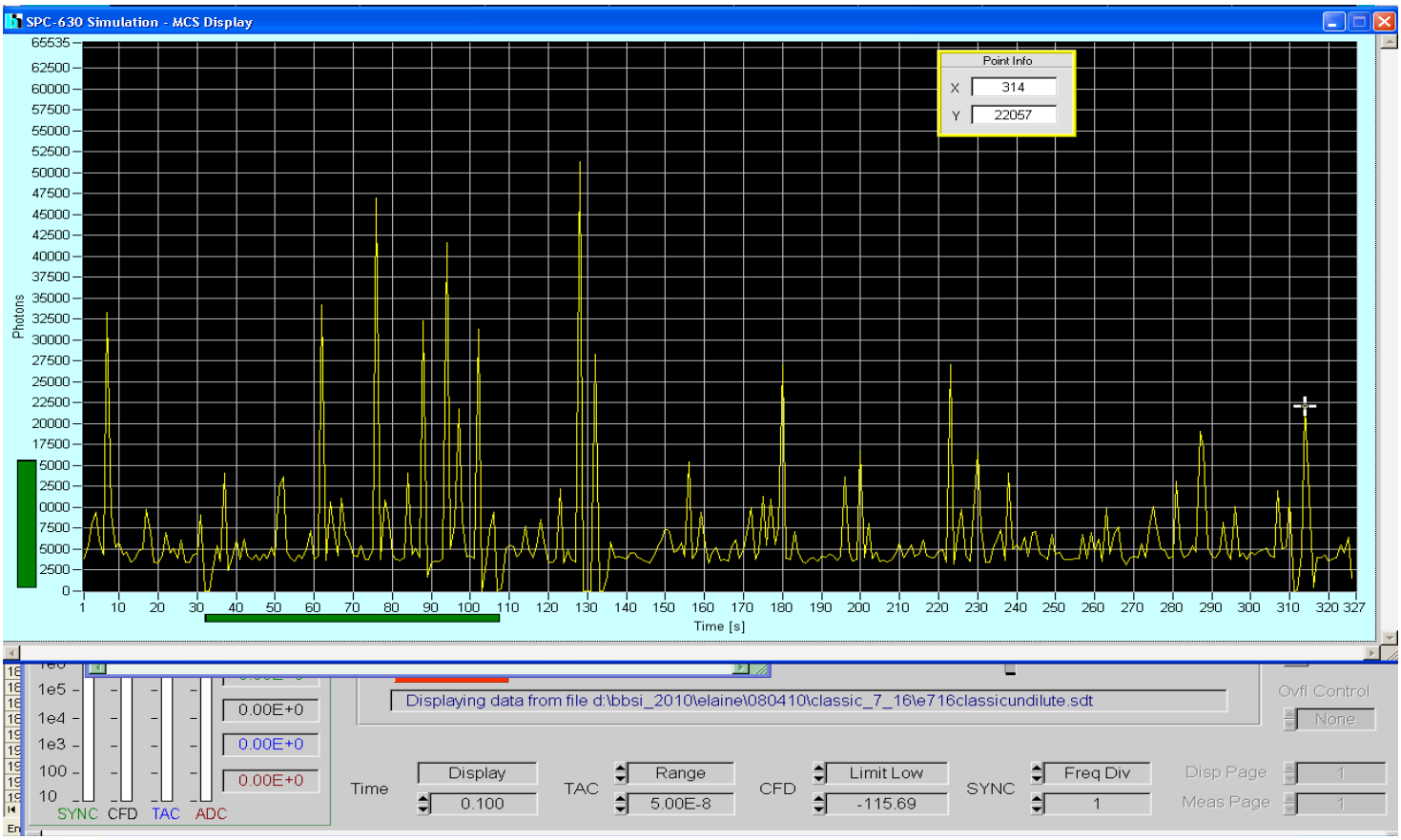

Figure D.8 MCS for siRNA-nanoliposomes sample 2, trial 4

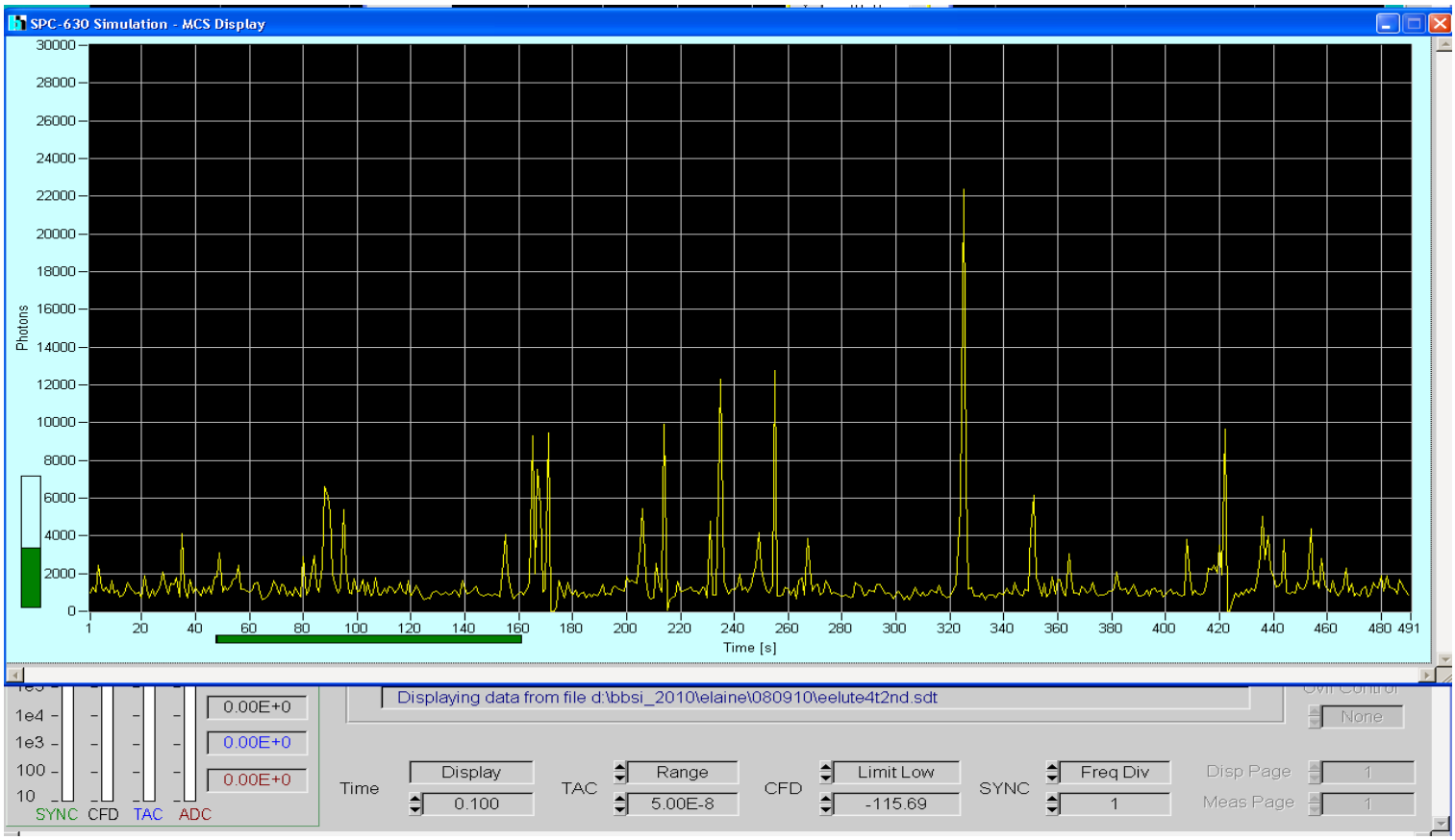

Figure D.9 MCS for siRNA-nanoliposomes sample 3, trial 1

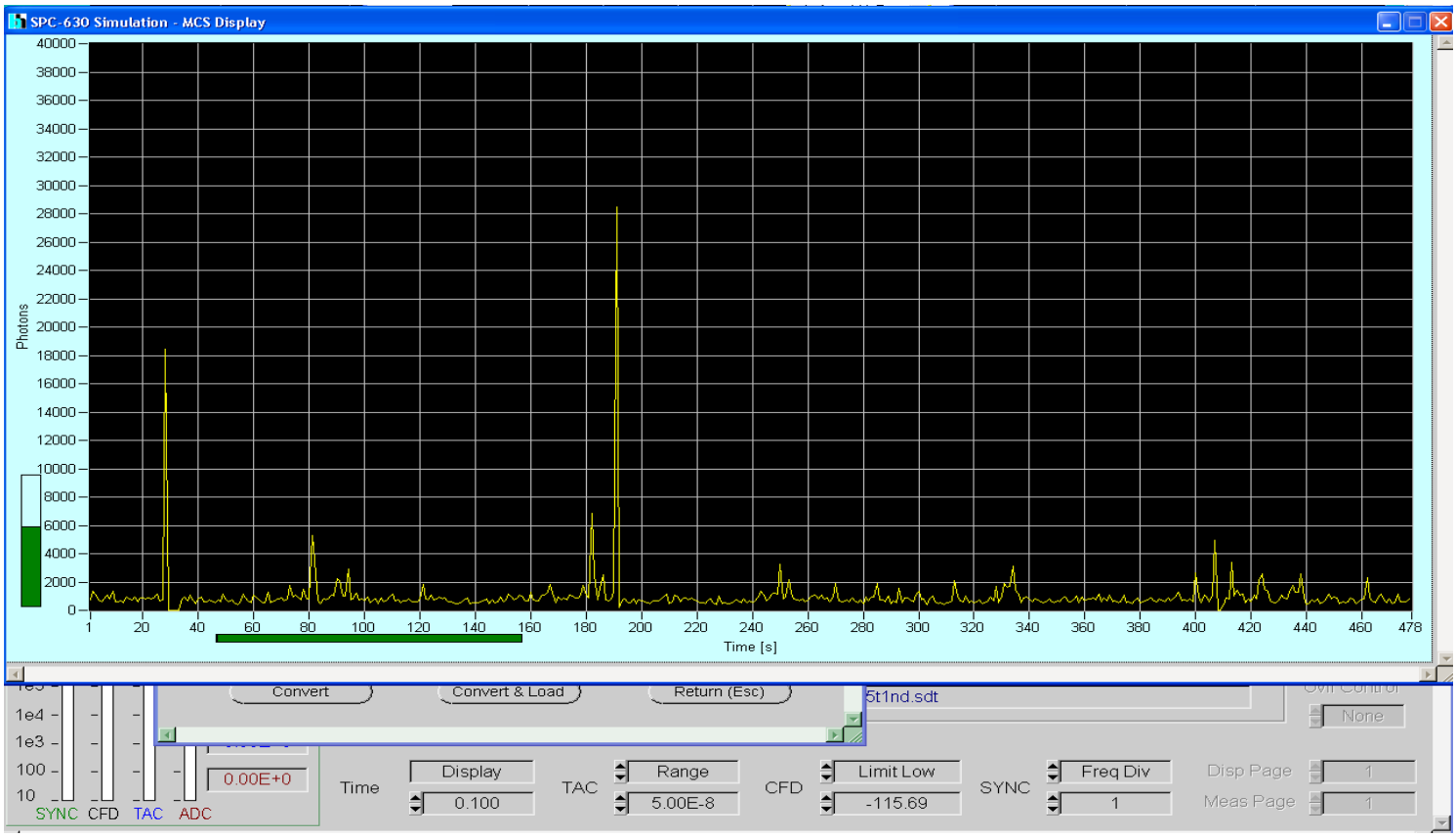

Figure D.10 MCS for siRNA-nanoliposomes sample 3, trial 2

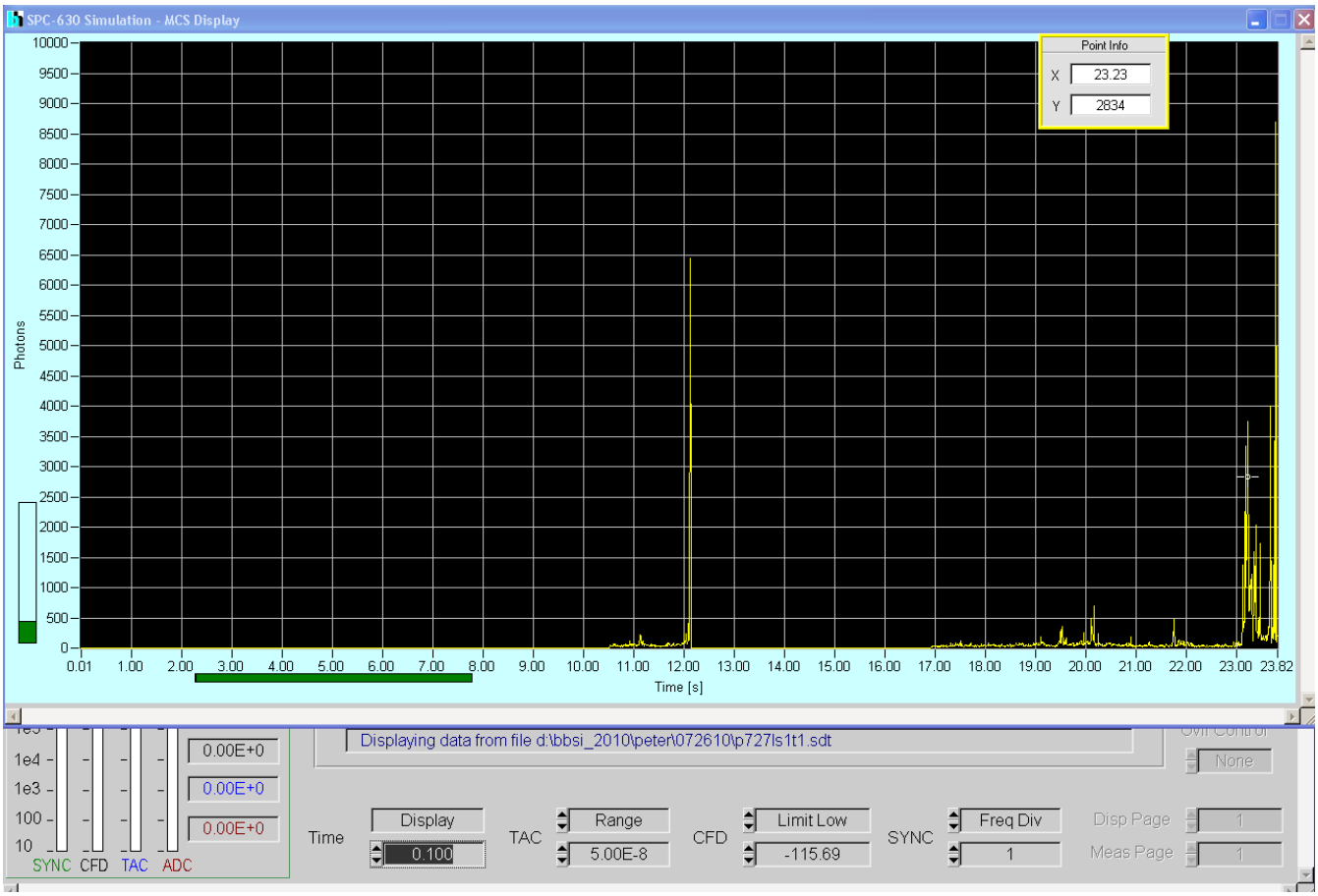

Figure D.11 MCS for siRNA-nanoliposomes sample 3, trial 3

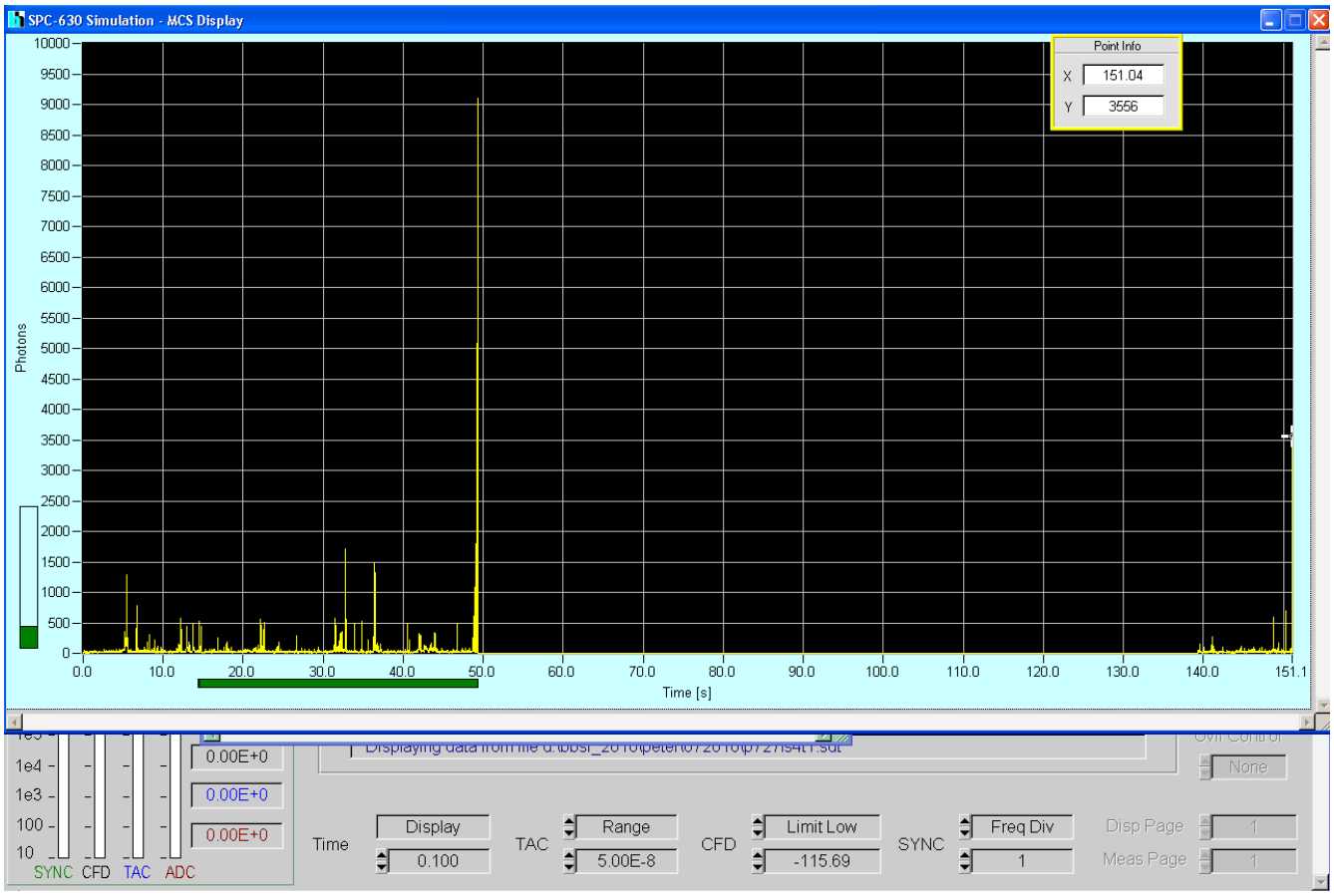

Figure D.12 MCS for siRNA-nanoliposomes sample 3, trial 4

References

1. Jemal A, Siegel R, Xu J and Ward E. Cancer Statistics 2010. *CA: Cancer Journal for Clinicians*. 60:5:277-300, 2010.

2. Becker W. *The bh TCSPC Handbook.* Berlin: Becker & Hickl GmbH, 2008.

3. Buyens K, Demeester J, De Smedt SS and Sanders NN. Elucidating the encapsulation of short interfering RNA in PEGylated cationic liposomes. *Langmuir* 25: 9: 4886-4891, 2009.

4. Chrai SS, Murari R and Ahmad I. Liposomes (a Review), Part One: Manufacturing Issues. 28, 2002.

5. Dittmar T, Heyder C, Gloria-Maercker E, Hatzmann W and Zanker KS. Adhesion molecules and chemokines: the navigation system for circulating tumor (stem) cells to metastasize in an organ-specific manner *Clin.Exp.Metastasis* 25: 1: 11-32, 2008.

6. Gullapalli RR, Tabouillot T, Mathura R, Dangaria JH and Butler PJ. Integrated multimodal microscopy, time-resolved fluorescence, and optical-trap rheometry: toward single molecule mechanobiology. *J.Biomed.Opt.* 12: 1: 014012, 2007.

7. Maherani B, Arab-Tehrany E, R. Mozafari M, Gaiani C and Linder M. Liposomes: A Review of Manufacturing Techniques and Targeting Strategies *Current Nanoscience* 7: 3: 436 <last_page> 452, 2011.

8. Mozafari MR. Nanoliposomes: preparation and analysis *Methods Mol.Biol.* 605: 29-50, 2010.

9. Schroeder A, Levins CG, Cortez C, Langer R and Anderson DG. Lipid-based nanotherapeutics for siRNA delivery. *Journal of Internal Medicine* 267: 9, 2009.

10. Schwille P and Haustein E. Fluorescence Correlation Spectroscopy An Introduction to its Concepts and Applications. *Biophysical Society* 94: 3: 1, 2009.

11. Semple SC, Akinc A, Chen J, Sandhu AP. Rational design of cationic lipids for siRNA delivery *Nat.Biotechnol.* 28: 2: 172-176, 2010.

12. Tokatlian T and Segura T. siRNA applications in nanomedicine. *Wiley Interdiscip.Rev.Nanomed Nanobiotechnol* 2: 3: 305-315, 2010.

13. Torchilin VP. Recent advances with liposomes as pharmaceutical carriers *Nat.Rev.Drug Discov.* 4: 2: 145-160, 2005.

Elaine Marie Tanella

17 Wyatt Rd Garden City, NY 11530
e.tanella@gmail.com
516.330.1755

EDUCATION

The Pennsylvania State University — Anticipated Graduation: May 2012
Schreyer Honors College
Bachelor of Science in Bioengineering
Minors in Italian & Biology

International Summer Program on Differential Equations, Beijing, China — Summer 2009
Joint Pennsylvania State University and Peking University Program
- Selected by the Math Department as one of 14 students to participate in this joint program
- Worked in collaborative groups with Chinese classmates to create presentations regarding the implementation of numerical techniques for analysis of ordinary and partial differential equations

Thesis Title: The use of time correlated single photon counting to optimize siRNA encapsulation in nanoliposomes
Thesis Advisor: Dr. Peter Butler, Department of Bioengineering

AWARDS

Dean's List
Academic Excellence Scholarship
Waltemeyer Howard Senior Scholarship
Skull and Bones Honor and Tradition Society
Lion's Paw Senior Society

WORK EXPERIENCE

Auxiliary Business Services Marketing Intern — June 2011 – Aug. 2011
- Conducted market research in pricing, branding and merchandising of products
- Critiqued and provided recommendations for current social media efforts

College of Engineering Undergraduate Teaching Intern — Jan. 2011 – May 2011
- Served as the sole teaching intern for the Cellular and Molecular Bioengineering course
- Held weekly office hours for a class of 80 students
- Graded all homework assignments and short answer portions of exams

Nanomedicine Research Laboratory — Mar. 2010 – May 2011
- Developed an appropriate technique for nanoliposome fabrication
- Analyzed the mechanical properties of the nanoliposomes using time correlated single photo counting
- Evaluated the encapsulation efficiency of siRNA using the developed nanoliposome formulation method

Cardiovascular Tissue Engineering Laboratory Aug 2009 – Dec. 2009

- Assessed various research papers regarding tissue engineering of bioprosthetic heart valves
- Discussed potential research topics relating to the construction of bioprosthetic heart valves

LEADERSHIP EXPERIENCE

Penn State Dance Marathon (THON)

- Overall Chairperson Mar. 2011 – Mar. 2012
  - Responsible for the execution of the largest student-led philanthropy in the world
  - Selected 15 Overall Committee Members (Board of Directors), overseeing 315 Captains (Project Managers) and 3,300 Committee Members (Project Leads)
  - Works closely with University Administrators and the Penn State Office of Annual Giving to develop and implement effective fundraising strategies
  - Serves as the official spokesperson and liaison to all supporters worldwide, including alumni, media, and corporate donors
  - Oversees and coordinates the logistics for a two day dance marathon with more than 5,000 participants and 12,000 spectators
  - Record 2012 total of $10.68 million was a 11% increase from the 2011 total of $9.56 million
  - To date, THON has raised more than $89 million for The Four Diamonds Fund, which supports families battling pediatric cancer and innovative research at the Penn State Hershey Medical Center
- Overall Communications Chairperson Apr. 2010 – Apr. 2011
  - Responsible for the development of all communication strategies, including web content and execution among students, faculty, staff, community members and alumni
  - Wrote and managed a weekly newsletter for more than 20,000 subscribers
  - Directed a committee of 24 Captains and 180 Committee Members
  - Advised several hundred organizations and prospective volunteers regarding their fundraising efforts and involvement

Pennsylvania Literacy Corps Tutor Jan. 2010 – May 2010

- Tutored an English as a Second Language student for 45 hours educating the student on general English language principles and American culture

Penn State Fresh Start Team Leader Aug 2009

- Led a group of 20 freshman students at a service site and assisted in their freshman year acclimation process